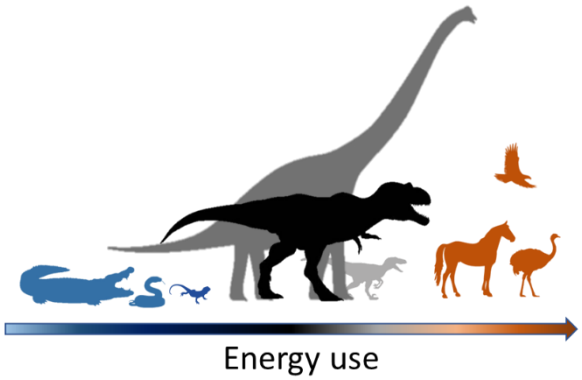

Molecular evolution of vertebrate genes involved in mitochondrial biogenesis: unravelling the origins of birds' endothermy

Hugo da Costa Moreno
Biodiversity, Genetics and Evolution
CIBIO-InBIO/BIOPOLIS
2022

Supervisor
Prof. Agostinho Antunes, FCUP and CIIMAR

Co-supervisor
Dr. Tito Mendes, ENS-Lyon


cibio


ciimar


U.PORTO
FACULDADE DE CIÊNCIAS
UNIVERSIDADE DO PORTO

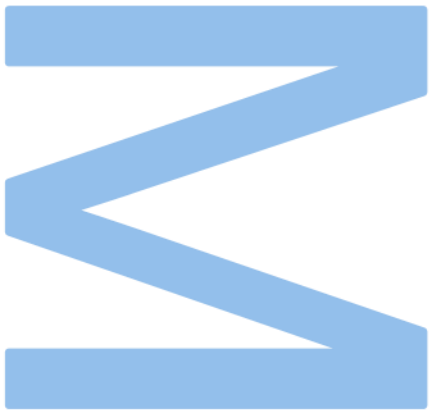

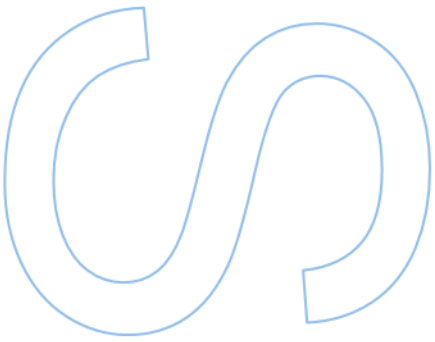

Sworn Statement

I, Hugo da Costa Moreno, enrolled in the Master Degree Biodiversity, Genetics and Evolution at the Faculty of Sciences of the University of Porto hereby declare, in accordance with the provisions of paragraph a) of Article 14 of the Code of Ethical Conduct of the University of Porto, that the content of this dissertation reflects perspectives, research work and my own interpretations at the time of its submission.

By submitting this dissertation, I also declare that it contains the results of my own research work and contributions that have not been previously submitted to this or any other institution.

I further declare that all references to other authors fully comply with the rules of attribution and are referenced in the text by citation and identified in the bibliographic references section. This dissertation does not include any content whose reproduction is protected by copyright laws.

I am aware that the practice of plagiarism and self-plagiarism constitute a form of academic offense.

Hugo da Costa Moreno

30/09/2022

Acknowledgements

First and foremost, I want to express my deepest gratitude to my supervisor, Agostinho Antunes whose support helped me achieve my best potential.

A special thanks to my co-supervisor Tito Mendes for his insightful opinions and incisive feedback during all the steps of the thesis, from the planning of the procedures to the improvement and discussion of the written thesis. His knowledge of the subject and his pertinent questions resulted in reflections that ended up culminating in great improvements to the work. Also, by encouraging me to learn and test new methodologies he magnified my learning potential, which I am certain will continue to be fruitful in the future and continue to help me improve professionally.

I am also grateful to Luana Ramos, Liliana Silva, and Manuel Seixas for all their keen commentaries and during the work, which helped improve the quality of the current thesis. Additionally, I would also like to thank my other EGB colleagues for their occasional help and support.

Lastly, I must acknowledge my family for their patience. Their confidence in me was of great help in maintaining my resilience and focus.

This work was partially supported by the FCT project PTDC/CTA-AMB/31774/2017 (POCI-01-0145-FEDER/031774/2017).

Resumo

A hipótese mais consensual na comunidade científica sobre a evolução da endotermia sugere que esta evoluiu múltiplas vezes em várias linhagens de forma independente. Esta fisiologia é atualmente predominante em aves, mamíferos, e também em algumas linhagens de repteis e peixes. As aves e os mamíferos são endotérmicos na totalidade do seu corpo, tendo desenvolvido as taxas metabólicas e temperaturas corporais mais elevadas entre vertebrados. O desenvolvimento destas e outras características diferenciadoras permitiu-lhes expandir os seus nichos térmicos e aumentar os seus níveis de atividade e taxas de reprodução. Considerando o papel da mitocôndria no metabolismo celular e produção de energia, é provável que algumas características diferenciadoras das mitocôndrias de organismos endotérmicos tenham tido elevada importância na aquisição da endotermia. Desta forma, mutações nos genes que regulam a função mitocondrial podem ter sido algumas das alterações moleculares que foram selecionadas e promoveram a transição para a endotermia.

Considerando esta hipótese, foram extraídas sequências nucleotídicas de genes que regulam a função mitocondrial a partir de genomas de aves e répteis. Estas foram usadas em várias análises bioinformáticas de genómica comparativa para avaliar as suas pressões seletivas e comparar as métricas genéticas destes genes com características fenotípicas associadas à endotermia.

As elevadas pressões seletivas e a potencialmente elevada expressão encontrada nos genes das aves corroboram o papel mitocondrial na aquisição da endotermia e possivelmente representam algumas das alterações genómicas na base da transição para esta fisiologia. Em sentido oposto ao inicialmente esperado, foram detetadas pressões seletivas elevadas, juntamente com índices de expressão potencialmente elevados, na linhagem dos Crocodylia e nos ancestrais das aves, os dinosauros. Estes resultados sugerem que, tal como sugerido em trabalhos recentes, os dinossauros apresentariam um perfil endotérmico, podendo ter ocorrido uma reversão para a ectotermia em crocodilos.

Palavras-chave: homeostase térmica, genómica comparativa, bioenergética, regulação mitocondrial, termorregulação

Abstract

Endothermy is supposed to have evolved multiple times independently in different lineages. This physiological trait is currently predominant in birds and mammals, but also occurs in some reptile and fish lineages. However, mammals and birds display whole-body endothermy and have evolved the highest metabolic rates and body temperatures among the extant animals. The development of these differentiating traits allowed them to expand their thermal niches, increase their activity levels and reproductive rates. Considering the role of the mitochondria in metabolism and energy production, some of the mitochondrial differences found in endotherms likely played roles in the acquisition of endothermy. Therefore, mutations in the genes regulating the mitochondrial function could have been selectively fundamental for the transition to endothermy.

Considering such hypothesis, nucleotide sequences of genes that regulate mitochondrial function were extracted from birds and reptile genomes. These were used in detailed comparative genomic analyses, aiming to assess selective pressures on synonymous and non-synonymous mutations and evaluate the association between genetic and phenotype traits associated with endothermy.

The high selective pressures and potential high gene expression levels in birds support the role of mitochondrial regulatory genes in the acquisition of endothermy and might represent some of the genomic changes behind the transition to this physiology. Interestingly, the high selective pressures and potential expression levels found in the Crocodylia lineage and the avian ancestors (dinosaurs) may imply, in agreement with recent studies, that endothermy already occurred in dinosaurs, while crocodiles underwent a reversion to ectothermy.

Keywords: thermic homeostasis, comparative genomics, bioenergetics, mitochondrial regulation, thermoregulation

Table of Contents

List of Tables

List of Figures

Attachments

List of Abbreviations

ATP	ADENOSINE TRIPHOSPHATE
ANT	ADENINE NUCLEOTIDE TRANSLOCASE
UCP	UNCOUPLING PROTEIN
N50	THE SEQUENCE LENGTH OF THE SHORTEST CONTIG AT 50% OF THE TOTAL GENOME LENGTH
MEGA7	MOLECULAR EVOLUTIONARY GENETICS ANALYSIS VERSION 7.0
DAMBE7	DATA ANALYSIS IN MOLECULAR BIOLOGY AND EVOLUTION V7.2.25 SOFTWARE
GARD	GENETIC ALGORITHM FOR RECOMBINATION DETECTION
PAML	PHYLOGENETIC ANALYSIS BY MAXIMUM LIKELIHOOD SOFTWARE PACKAGE V4.8
LMAP	LIGHTWEIGHT MULTIGENE ANALYSES IN PAML V1.0.2 SOFTWARE
DNASP	DNA SEQUENCE POLYMORPHISM
LTR	LIKELIHOOD-RATIO TEST
PSS	PUTATIVE POSITIVE SELECTED SITES
CUB	CODON USAGE BIAS
CAI	CODON ADAPTATION INDEX
ENC	EFFECTIVE NUMBER OF CODONS
RSCU	RELATIVE SYNONYMOUS CODON USAGE
SCHI2	SCALED CHI SQUARED
GC	PERCENTAGE OF GUANINE AND CYTOSINE BASES OF EACH GENE OR GC CONTENT
GC3	GC CONTENT AT THE THIRD CODON POSITION
ANOVA	ANALYSIS OF VARIANC
BMR	BASAL METABOLIC RATES
AICC	CORRECTED AKAIKE INFORMATION CRITERION
DS	SYNONYMOUS SUBSTITUTION RATES
DN	NON-SYNONYMOUS SUBSTITUTION RATES

1.Introduction

Birds consist of a highly diverse group of vertebrates with great morphological and behavioural diversity [1-4] that occupy a wide range of ecological niches [1, 4]. All bird species descend from the theropod dinosaur lineage [5] (Figure 1), which diverged from other dinosaurs 165 million years ago [1]. However, the avian radiation that culminated in the current diversity only occurred after the Cretaceous-Paleogene mass extinction, which is estimated to have ended 75% of the life forms on earth, approximately 65 million years ago [6]. Only a few bird lineages were able to survive such mass extinction [2, 5], alongside mammals, which colonized new habitats and niches, previously dominated by dinosaurs. Consequently, this promoted the radiation and diversification of modern birds [7], which can be currently subdivided into Paleognathae, Galloanserae and Neoaves [3, 8, 9] (Figure 1).

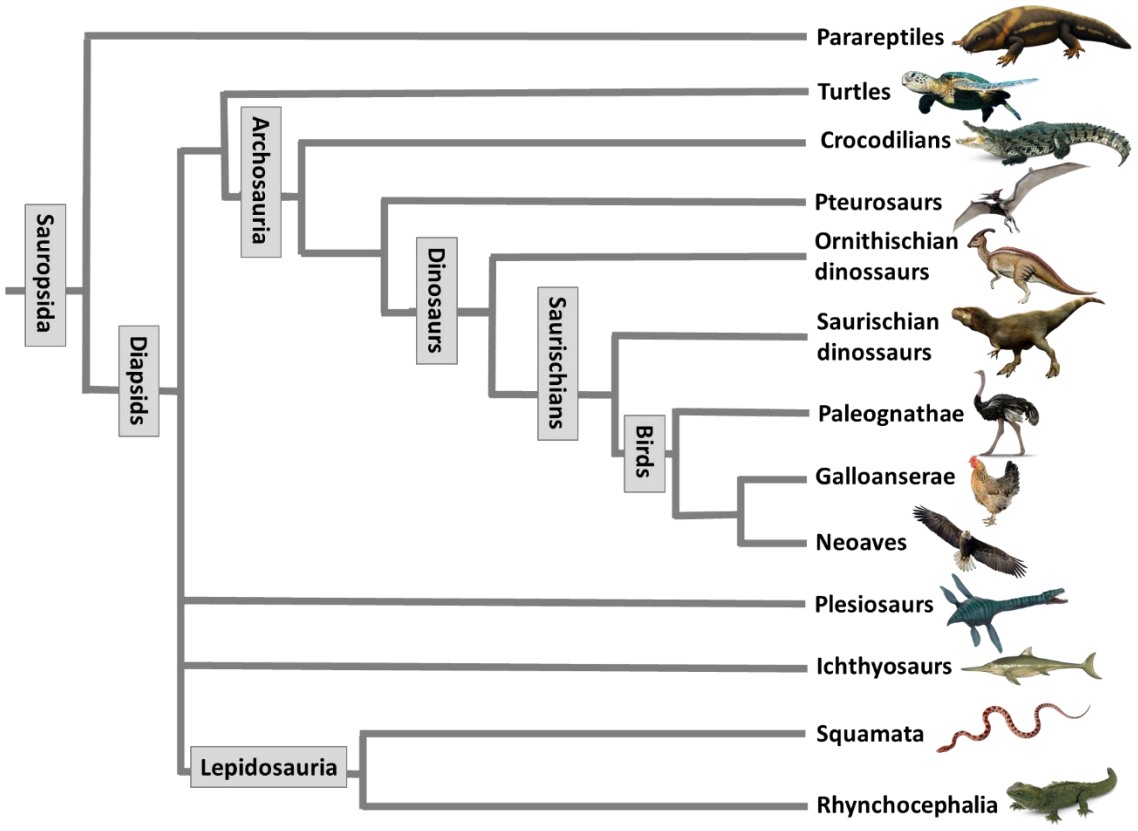

Figure 1 - Phylogenetic relationships among the major Sauropsid clades.

Alongside mammals, birds are the taxa most associated with endothermy, a physiological state characterized by the production of heat via metabolic processes [10, 11]. However, this physiological state is currently assumed to have evolved independently, multiple times on different taxa and is also present in some fishes [12,

13], reptiles [14, 15] and increasing evidences also support its presence in dinosaurs [16, 17], implying an earlier acquisition in the lineage that gave origin to birds [17]. A recent study has also argued for an early occurrence of endothermy in Amniotes, thus making endothermy a plesiomorphy of this taxon that was later lost in the extant reptile lineages [17]. Contrary to this argument, there have been works that reported no evidence of endothermy in ancestral synapsids and instead detected a gradual transition to endothermy within the synapsids [18]. Nevertheless, the physiologies of birds and mammals are unique. In addition to homeothermic endothermy, an endothermy physiology in which the individual can maintain stable internal body temperatures [19, 20], these taxa also exhibit various other physiological differentiating factors, when comparing to reptiles. Their superior mitochondrial density and efficiency, increased body temperatures (which are among the highest within vertebrates) [21-23], and superior metabolic rates [24], oxygen transport capacity [23, 25], aerobic activities [26] and muscle mass [24, 26] are just some of the several interlocked factors which relate to the acquisition of endothermy in mammals and birds, and distinguish them from reptiles [17]. For example, the higher mitochondrial densities and efficiency might have played a role in the increase of the metabolic rates [27], which allowed body temperatures to increase and promoted the development of whole-body homeothermic endothermy [28, 29]. Similarly, the increase of the oxygen transport capacity, due to increased heart rates and blood pressures, would support the high oxygen consumption of aerobic metabolism, allowing the increase of the metabolic rates [23, 25].

The emergence of homeothermic endothermy in birds and mammals was likely one of the factors that supported their successful radiation and promoted the occupation of new thermal and geographical niches [10]. This niche expansion was potentiated by the multiple morphological and ecological advantages that resulted from the acquisition of this physiological state, such as the increase of the individual's muscular power output and activity levels, the development of more thermally stable environments for enzymatic reactions, the complexification of the nervous system and the increase of the reproductive rates [10, 30].

Despite the higher maintenance costs of endothermy [31, 32], which can be difficult to cope with, since a higher intake of food, water and oxygen is necessary [11, 26, 31], at least one of its long-term advantages was so impactful to the species fitness that the development of this energetically costly physiology was favoured by strong selective pressures [12]. Based on this concept, multiple hypotheses have been proposed, aiming to explain the evolution of this physiological state [23, 33], including the niche expansion [34], the body size miniaturization [35], the aerobic capacity [28, 29]

and the parental care hypotheses [36, 37]. A more recent hypothesis takes all the advantages of endothermy in consideration and proposes that this physiological trait has evolved gradually and independently in three different phases in birds and mammals [33]. According to this triphasic model, the increased endothermic profile, expressed as increases of the metabolic rates and body temperatures, would have occurred firstly as a response to the benefits of parental care and higher activity levels. In a second phase, the increased endothermic profile resulted from increased thermoregulation, associated with body size miniaturization, which was showed to be the path of least resistance to the development of endothermy. According to this argument the energy saved by the decrease in size would allow the development of a higher cost physiology as endothermy, with the costs of being large being trade for those of endothermy [38]. Additionally, in the second phase the increment would also occur with the improvement of the insulation, associated with the development of fur and feathers [33]. At last, the increases of body temperature would have occurred in pulses associated with the development of flight in birds and due to the adaptation to the Cenozoic environmental cooling [33].

Still, the aerobic capacity model, which proposed that endothermy evolved as a by-product, is currently one of the most accepted [10]. It suggests that natural selection on physiological factors for increased aerobic capacity and sustained levels of activity led to the increase of the maximal aerobic capacity [28], which promoted the elevation of the basal metabolic rate [29]. Considering these models, the elevation of the metabolic rates behind the rise of endothermy, could have resulted from the increment of the mitochondrial densities and efficiency. These increases would result in higher ATP production rates that would allow the individuals to develop elevated metabolic rates. Furthermore, the increment of the mitochondrial membrane leakage, characteristic of endotherms, also led to an increase of heat production, through direct proton dissipation across the membrane or the uncoupling mechanism, using intermembrane proteins such as the adenine nucleotide translocases (ANTs) and the uncoupling proteins (UCPs) [39]. By leaking protons across the mitochondrial inner membrane, these pathways dissipate proton motive force as heat, instead of storing the energy as ATP through synthesis [40].

Overall, as the cell energetic central organelles, crucial to the cellular metabolism and energy production [41, 42], mitochondria should have played a role in the increase of the metabolic rates [41, 43], which allowed for the increase in energy and heat production and, ultimately, the evolution of endothermy [43, 44]. Therefore, changes in the genes that regulate the mitochondria should have significant impacts on the species fitness and thus, by natural selection, affect the species evolution. Hence, the genes that

regulate the mitochondrial function (Table S1) are expected to be subjected to higher selective pressures in the avian class than in their reptilian ancestors. For this reason, the aim of this project was the assessment of these genes, in order to assess them in the Sauropsid lineage and compare the selection patterns in the four Sauropsid clades to shed some light into the ectothermy-endothermy transition in the lineage.

To summarize, I aimed to evaluate the evolution of the genes that regulate the mitochondrial function and use that information to help identify the evolutionary origin of endothermy in the Sauropsid lineage.

The results presented in this study support the role of *PPARG* and *PPARGC1B*, two crucial genes to the mitochondrial regulation, on a gradual development of endothermy. Besides *PPARG*, the positive selected sites found in *MIC13*, *ND1* and *ND5*, genes with roles on mitochondrial dynamics and oxidative phosphorylation, could also have been some of the molecular change behind the transition to endothermy. At the same time, the potential higher gene expression levels of *DNM1L*, *PPARGC1B*, *PRKAA2* and *MIEF1* are also indicative of a mitochondrial influence in the development of an endothermic profile. The elevated number of genes under selection in the crocodiles might also be an indication of a return to ectothermy in this taxon, with the mutations found potentially being the reversion of the changes that allowed the development of endothermy.

2. Materials and Methods

2.1. Gene identification

A primary search for genes that participate in the mitochondrial regulation and functioning was done resorting to the Gene Ontology database [45, 46] and using the following search terms: mitochondrial fusion, mitochondrial fission, mitophagy and mitochondrial organization. The obtained list was complemented and confirmed with a thorough revision of literature, which was done to find evidence of the association with mitochondrial functions, including mitochondrial biogenesis, fusion, fission and motility, mitochondrial quality control, transcription, protein import, oxidative phosphorylation and mitochondrial membrane leakage. The literature research resulted in a list of 78 genes with reviewed and published information about their roles in the various mitochondrial functions previously referred (Table S1).

2.2. Sequence collection

The Sauropsid lineage, which includes birds and reptiles, was chosen to access the transition from ectothermy to endothermy, because, contrarily to Synapsids, this lineage still possesses extant ectotherm and endotherm representatives, and birds are the endotherms with highest body temperatures and metabolic rates [47]. Prior to the gene extraction, a search for avian and reptilian genomes was conducted in the GenBank database [48]. For birds, only the genomes of the two most basal groups were selected (Paleognathae and Galloanserae clades), in order to increase the resolution towards the ectothermy-endothermy transition, while avoiding bias related to other traits of this lineage (e.g., re-acquisition of flight in Sauropsids). For reptiles, genomes of species of each of the four extant orders were selected, in order to accurately represent the reptile diversity. Therefore, a set of 55 avian genomes and 60 reptilian genomes was selected (Tables S2 and S3), balancing the comparative assessment between reptile and bird's species. The range of contig N50 of birds' and reptiles' assemblies is shown in Figure 2.

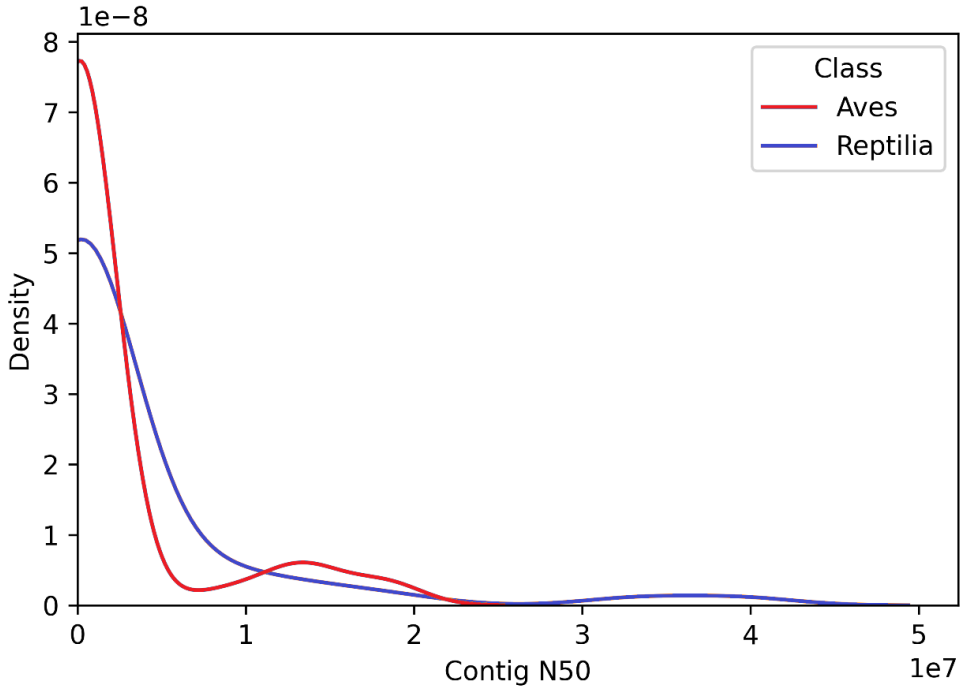

Figure 2 - Distribution of contig N50 of the assemblies used in this work.

For each of the selected genes, appropriate protein sequences to be used as queries in the gene extraction were downloaded from the UniProtKB database [49], with preference given to the sequences presenting the highest quality. In general, the protein sequences of *Gallus gallus* were used as references for the bird genomes, but queries

from alternative avian species were also used when *G. gallus* sequences were not available (Table S4). For reptiles, different reference queries were used for each taxonomic order, due to the great genetic divergence among them. The protein sequences used as reference were in general from *Anolis carolinensis* (Squamata and Rhyncochephalia), *Crocodylus porosus* (Crocodylia) and *Chelonia mydas* (Testudines). Despite the preference for this reference query, alternative queries were used for several genes (Table S5), when protein sequences were not available, or if the available reference protein was incomplete or presented low quality.

The sequence search was performed primarily in the GenBank database [48], using the tBLASTn tool [50] and employing the collected protein queries (Tables S4 and S5). When multiple sequences were available for the same species, the sequences presenting the lower e-values and higher query coverage were selected. However, this only allowed the collection of a limited number of sequences, for a restricted number of species. Consequently, the remaining sequences were searched in genomes available in GenBank (Tables S2 and S3) using the protein2genome option available in the Exonerate tool [51], and the same protein sequences as queries.

2.3. Multiple sequence alignments and sequence quality control

Quality control steps were performed to improve the quality of the dataset and avoid the use of problematic sequences. Sequences presenting intrasequential stop codons or reading frame shifts were considered pseudogenes and were removed from the corresponding datasets. For each identified pseudogene, location and details of these mutations were registered (Table S6), to study the pseudogenization events, which can reveal much about the direction in which the selective pressures have acted [52]. Each exonerate output was assessed, and the intron size and respective position in the gene were registered.

Posteriorly to this initial quality control, all orthologous sequences from each gene were aligned by codons using the algorithm ClustalW implemented in the Molecular Evolutionary Genetics Analysis 7.0 (MEGA7) software [53]. The alignments' quality was inspected to detect nucleotide ambiguities, since these cannot be properly interpreted by a considerable number of software, and they were removed from the sequences when found. The filtered datasets resultant from the manual quality control were then submitted to final alignments, employing the MAFFT algorithm implemented in the GUIDANCE 2.0 webserver [54, 55] with 100 bootstrap repeats. Only the columns with a confidence score above 0.93 were retained, thus excluding all the dataset positions that were considered unreliable [55]. Posteriorly, all alignments were manually refined.

2.4. Concatenation and saturation analysis

The multiple sequence alignments were concatenated in one dataset, using the Geneious 11.0.5 software [56]. Concatenation is important, since it allows the improvement of the power to estimate the phylogeny, by increasing the phylogenetic signal over noise ratio [57, 58], and consequently helps to achieve a phylogenetic reconstruction that is closer to a species tree than a gene tree, *i.e.*, to obtain a tree that represents the true phylogenetic relationships among the species [58].

Nucleotide saturation precludes phylogenetic algorithms to infer the ancestral state, thus leading to the underestimation of the sequences divergence [59] and rendering the reconstruction of the sequence's evolutionary relationships impossible. Considering this, in order to reduce the non-phylogenetic signal or noise [59], the nucleotide saturation of the dataset was estimated using the Xia's test [60] of the Data Analysis in Molecular Biology and Evolution v7.2.25 software (DAMBE7) [61].

2.5. Partition analysis and selection of nucleotide substitution model

Prior to the phylogenetic reconstruction, it is crucial to select the most suitable model of evolution, since an incorrect selection of the model and its parameters can lead to worse performances of the phylogenetic algorithms [62], affecting the resultant tree topology [63], branch lengths [64] and statistical support values [65]. Hence, if the heterogeneity of evolutionary characteristics in different genes is not considered, an inaccurate tree might be created [66]. Considering that different genes may display great variation in terms of evolutionary characteristics, the heterogeneity of the concatenated dataset should not be ignored. Therefore, two ways for the accountancy of heterogeneity in evolutionary processes is to employ mixture models or partition analysis [67]. While most partitioning methods demand the *a priori* selection of potential partitions [67, 68], in mixture models the application of a model to a site is directly determined from the data [67].

Therefore, to avoid the bias of the *a priori* selection of partitions and since there are evidences that the *a priori* selection often fails to account for the variation of patterns of evolution found in the sequences [68], the Genetic Algorithm for Recombination Detection (GARD) test [69] of the Datamonkey webserver [70] was used to search for potential recombination breakpoints. Considering that regions separated by the recombination breakpoints potentially have different patterns of evolution, these breakpoints were used to manually separate the dataset into 101 partition files. Then, the jModeltest v2.1.7 software [71] was used to calculate and select the best model of nucleotide substitution, for each one of the partitions, thus, considering the evolutionary

differences within the dataset and allowing each partition to receive different parameters and models for the phylogeny reconstruction.

2.6. Phylogeny reconstruction

Two phylogenetic trees were created and compared: a tree with a single model of evolution and a tree that considered the partitions. Both were created using the Maximum Likelihood algorithm, employing the IQTREE software v1.6.1 [72] with 10000 ultrafast bootstraps. The phylogenies were then edited in the Figtree software v1.4.4 [73, 74].

2.7. Selection analysis

Positive selection promotes the spread of beneficial genetic variants due to its impacts on the species fitness. A beneficial mutation will provide competitive advantage to the mutated individual, thus promoting the increase of its survivability and reproductive success. Such advantages will continue to be selected, leading to significant changes in population genetics, which generally occur rapidly under the influence of strong selective pressure [75]. Therefore, positive selection can be expected to be found where great changes exist between relatively close related taxa, and is thus important to reveal the genetic changes behind the evolution of a certain trait [75].

A search for positive selection was performed for each of the genes to compare the selection patterns of different Sauropsid groups and assess several evolutionary hypotheses. In order to detect positive selection, branch-site models of the CODEML software, implemented in the Phylogenetic Analysis by Maximum Likelihood software package v4.8 (PAML) [76, 77] were used with the Lightweight Multigene Analyses in PAML v1.0.2 software (LMAP) [78].

To ascertain if the individual gene alignments were appropriate to be used in selection analyses, DNA Sequence Polymorphism (DNASP v.6.12.03) [79] was used to calculate species pairwise values of synonymous substitution rates (*dS*). The values were used to assess the distribution of the *dS* values of each gene and to confirm if most values are distributed bellow the recommended maximum ($dS < 2$) to avoid compromising the estimates of *dN*/*dS* (ω) [80].

In the present work, selection analyses were used to test which genes present signatures of positive selection in each of the reptile orders and in birds, and which are the exclusive PSS behind these differences. Considering the paraphyletic profile of the Sauropsid lineage, several comparisons were performed. Besides the bird-reptile physiological dichotomy to test for the rise of endothermy in the avian lineage, there was

performed a comparison of Archosaur species with the Squamata and Testudines, in order to check for an earlier occurrence of endothermy at the base of the Archosauria and assess the recent hypothesis of a reversion to ectothermy in crocodiles [17] and occurrence of endothermy in several dinosaur lineages [16]. To further assess the endothermy of the avian ancestors, the dinosaurs, the occurrence of positive selection was also tested in the avian ancestral branch, located after the divergence of the Crocodilians from the avian class. To test the hypothesis of positive selection, the branch site models were used. These allow ω to vary between background and foreground branches. Thereafter the Null and Alternative models were compared, and the Likelihood-ratio test (LRT) values were calculated. For each model, three different replicates were performed, aiming to attain convergence among replicates. Discrepant replicates, with negative or large log-likelihood values were discarded. This approach allowed the above-mentioned comparisons of the selection rates between different Sauropsid clades for each of the selected genes and detect positive selection affecting sites in the selected foreground lineage. For the datasets with significant LRT ($P < 0.05$), for which the positive selection model is more suitable than the null model, putative positive selected sites (PSS) were inferred using the Bayes Empirical Bayes method, considering only the sites with significant posterior probabilities (PP > 0.95).

2.8. Evaluation of potential expression profiles

Codon usage bias (CUB), a phenomenon characterized by the differential use of synonymous codons, is also a consequence of mutation pressure and selection [81]. Changes in synonymous codons result in silent mutations. However, growing evidence shows that such changes have several impacts on transcription [82] and translation [83]. Thus, CUB has been reported to be a suitable proxy to the gene expression levels [82], with higher codon usage bias being found in highly expressed genes [84, 85].

In this study, CUB was used to evaluate the potential expression profiles of the genes that regulate the mitochondrial function. There is a great variety of CUB metrics, each considering the causes of CUB differently and being used to answer different questions [81, 85]. Considering the biological significance and potential implications of the occurrence of CUB, four indices were calculated for each of the genes to further assess the divergence between the mitochondrial regulatory genes in reptiles and birds (Table S7). The Codon Adaptation Index (CAI) allows the estimation of expression levels measuring the genes' bias towards a set of highly expressed genes. Other two metrics are the Effective Number of Codons (ENC), which calculates the absolute codon usage bias, *i.e.*, the total number of different codons used in a sequence, and the Scaled chi

squared (Schi2), which is the deviation of the use of a codon from balance use or absence of usage bias. The remaining metric, the Relative Synonymous Codon Usage (RSCU), is the codon-based measure of the relative codon usage bias values for each codon of a single amino acid. The calculation of the CAI demands the use of codon usage bias tables for highly expressed genes. Since ribosomal genes tend to have elevated expression levels across all tissues in vertebrates [86], codon usage bias tables of *Gallus gallus* and *Pogona vitticeps* nuclear ribosomal genes were extracted from the Codon Statistics Database [87] and used in the calculation. The RSCU results for amino acids coded by single codon (Tryptophane and Methionine, for the nuclear genes) and stop codons were excluded.

Additionally, because the variation in Guanine-Cytosine (GC) content and amino acid frequencies play a crucial role in determining synonymous codon choices [88-90] and the determination of gene expression levels, due to its correlation with codon usage bias [90], these metrics are usually used complementarily in codon usage bias analyses. Additionally, GC content is also associated with higher genome thermal stability [91] and tends to be higher in endotherms [92]. Thus, two additional metrics were also calculated, the percentage of guanine and cytosine bases of each gene or GC content (GC) and the GC content at the third codon position (GC3).

The GC3, GC, ENC, CAI, Schi2 and RSCU were calculated using DNASP, while the CAI, which has been used as a estimation of the theoretical gene's expression levels [93, 94], was calculated with the CAIcal webserver [95].

In general, the CUB metrics lack clear procedures to assess the statistical significance of the found biases [81]. Therefore, to overcome this limitation, parametric and non-parametric tests were used to identify which codons presented significantly higher codon usage bias in each of the Sauropsid clades. As was done in the selection analyses, multiple comparisons were performed to assess the mentioned evolutionary hypothesis. Considering that genetically close species tend to present similar codon usage patterns [96], significant variation is expected to be found not only within Sauropsida, but also within reptiles, because of the reptile paraphyly. Thus, to avoid bias caused by this variability, each of the reptile order was compared independently with the avian class. The ANOVA and Kruskal–Wallis tests were used in two comparisons: 1) the values of each codon were compared, to find the codons with significantly higher bias in each gene; 2) the results obtained for each of the Sauropsid groups under comparison were compared, to select codons with significant higher bias in each of the groups.

The overlap of the two comparisons allowed the selection of the significantly biased codons that have significant different codon usage patterns between birds and reptiles. Only the codons that presented significant differences in both parametric and non-parametric tests were considered to be under significant codon usage bias.

2.10. Genotype-phenotype correlations

The correlation between genetic data and phenotypic characters can be used to test hypotheses about their underlying evolutionary mechanisms, in order to infer how these traits evolved using ancestral sequences or to reconstruct the phenotypic evolution with both the phenotypic and molecular data [97]. In this work, the correlation between the molecular evolution of the genes related with mitochondrial functions and several traits associated with endothermy was assessed. In order to search for significant correlations between molecular data and quantitative traits, a search for traits related to endothermy in databases and literature was performed firstly. These traits included: 1) body temperature; 2) basal metabolic rates (BMRs); 3) biomass; 4) centroid latitude where the species occurs; and, 5) average annual environmental temperature the corresponding species was subjected. Information from several sources was compiled into Table S8. In addition, the difference between body temperature and ambient temperature was also calculated and used as a phenotype trait in the correlations.

Despite in-depth research, the information for the basal metabolic rate was reduced or absent for several species. In addition, the different sources of information used different metrics to express the metabolic rate, thus resulting in a higher number of missing values for this phenotypic trait. Hence, four metrics with different units were collected, each one presenting values for less than 20 species. Considering this, in order to use all the available information, all the BMR values were standardize and used in a new variable, with standard deviation units or z-scores as the new BMR metric [98].

For each pair of genotype/phenotype traits, Pearson correlation coefficient, Spearman's rank correlation coefficient and their respective *P*-values, were calculated using the SPSS v. 27.0.1.0 software [99].

3. Results

3.1 Data collection

A cumulative number of 8194 gene sequences were collected from the GenBank database and published genomes. Of these, 479 sequences were removed during the quality control, due to being either pseudogenized, too incomplete or highly divergent (Figure 3). The alignments of *FIS1, MTX1*, *MYC*, *PARIS*, *PERM1* and *SIRT4* were excluded due to high incompletion of the respective sequences, which reduced their alignment quality.

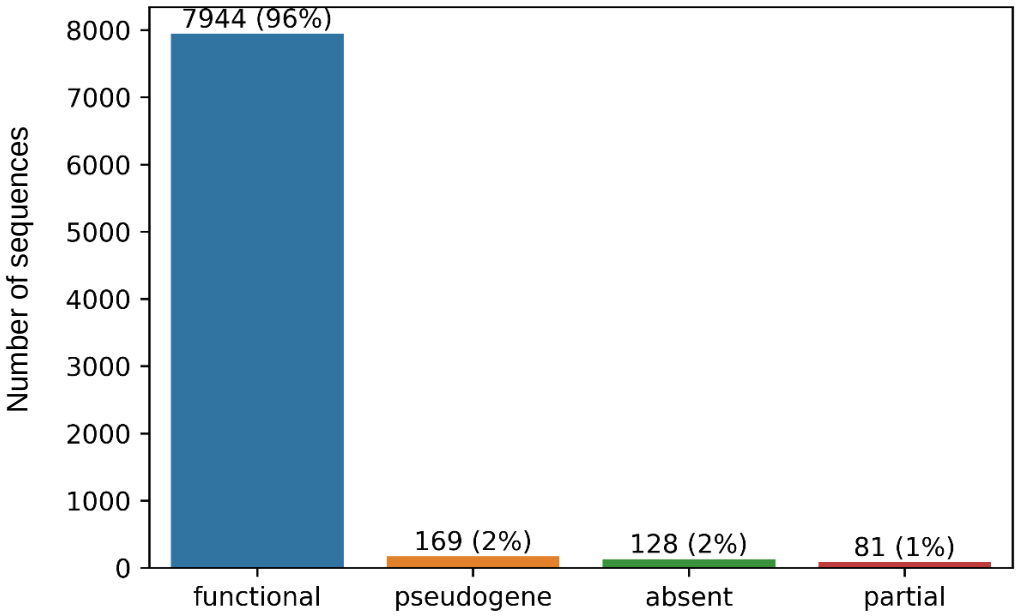

Figure 3 - Number and percentage of retrieved and excluded sequences during the dataset quality control.

No significant differences were found between the Sauropsid groups in terms of percentages of nonfunctional sequences (Figure 4B). The Contig N50 values of the diferent sauropsid groups were also statistically similar (Figure 4A). Genome quality did not correlate with the percentage of nonfunctional sequences (Figure 5).

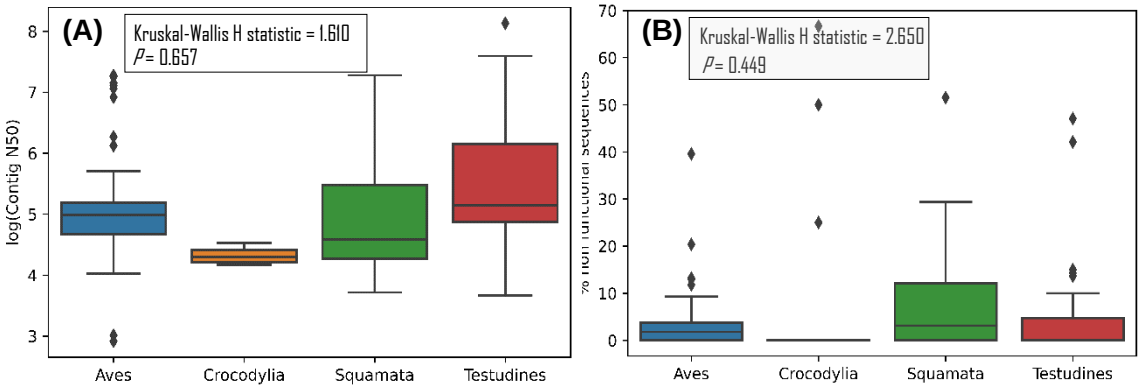

Figure 4 - Distribution of the genome Contig N50 (A) and percentage of non-functional sequences (B) in birds and reptiles. Non-functional sequences are those resultants from pseudogenization, or that are partial or absent for the species.

Considering the occurrence of pseudogenes for each gene, most genes displayed a higher number of non-functional sequences in reptiles than in birds (Figure 6). There were 45 genes where the reptiles showed a higher number of non-functional sequences. On the other hand, only 15 genes presented more non-functional sequences in birds than in reptiles.

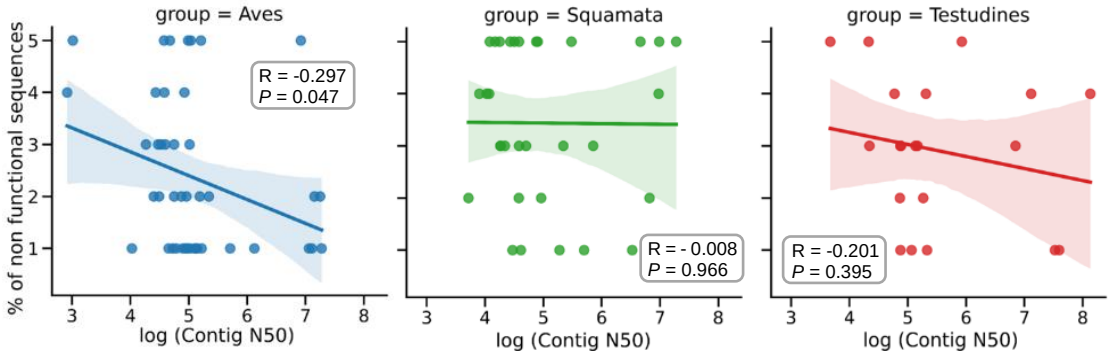

Figure 5 - Correlations between the assemblies Contig N50 and the percentage of non-functional sequences for each Sauropsid major group. Due to the low number of species the Crocodylia (N = 4) and Rhynchocephalia (N=1) are not represented. R = Pearson correlation coefficient.

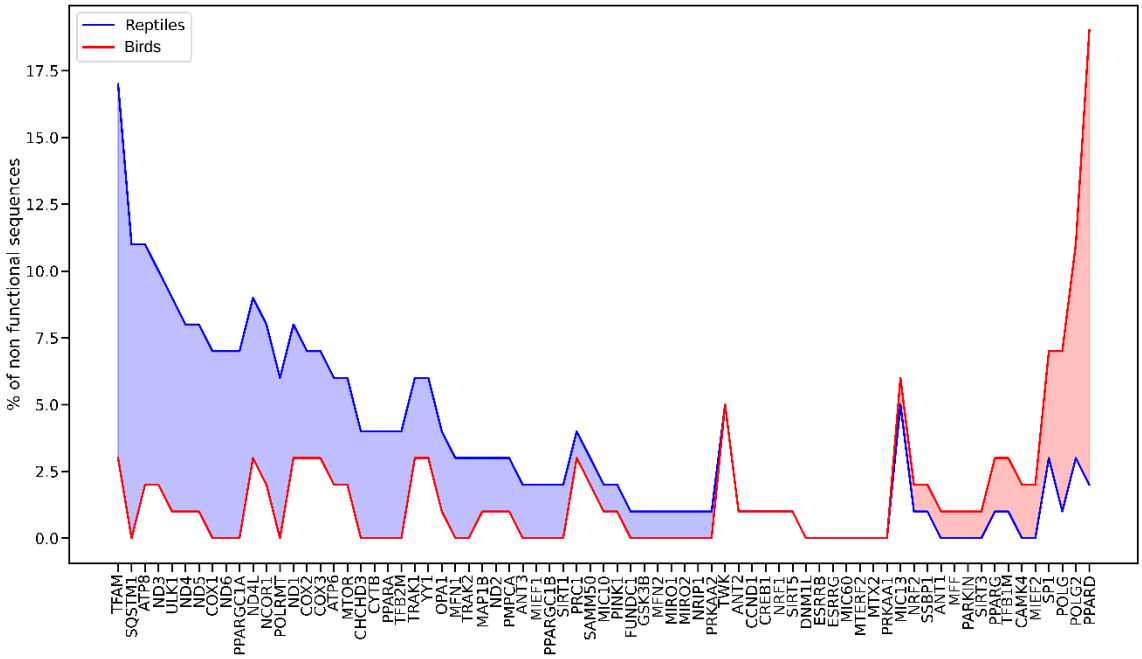

Figure 6 - Comparison of the percentages of non-functional sequences between birds and reptiles in each gene.

Considering each Sauropsid order individually, great variation can be found (Figure 7).

The Squamata are the taxa with the generally higher number of non-functional sequences.

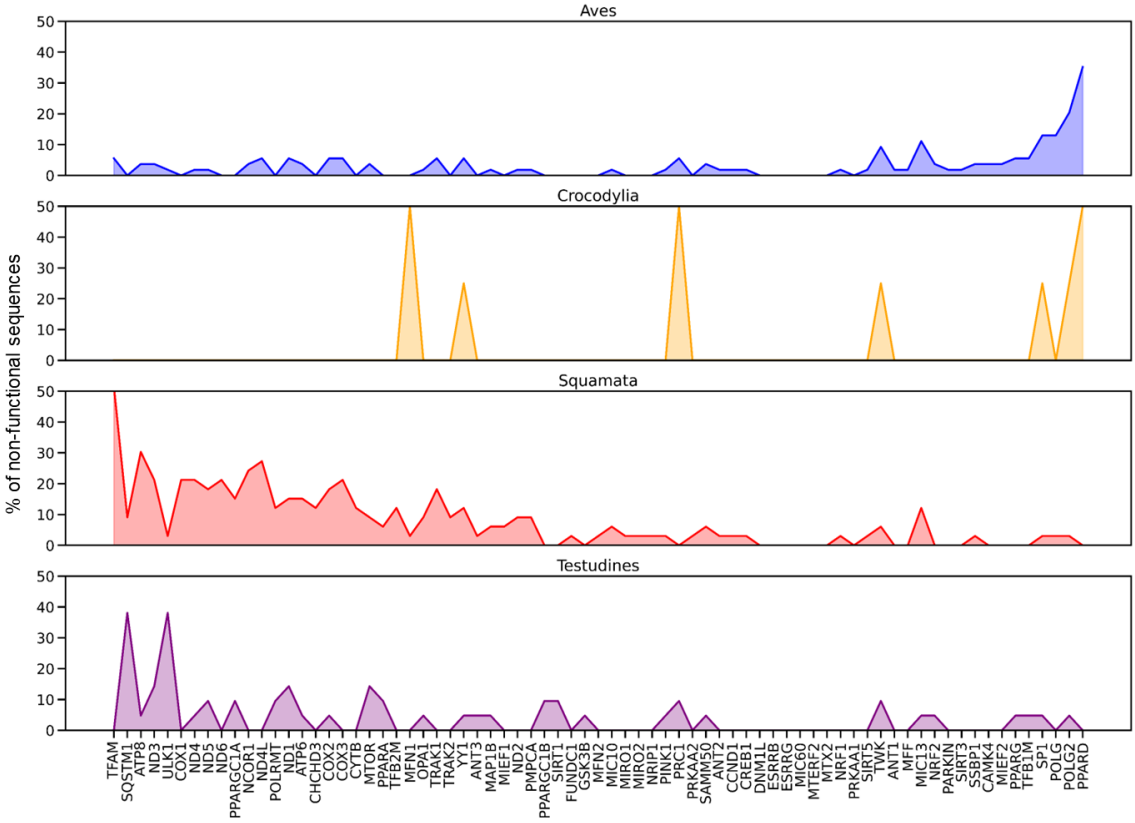

Figure 7 - Variation of the percentage of non-functional sequences between birds and the reptile orders.

However, the pseudogenization events are mostly random (Table S8), carrying no apparent connection to evolutionary changes associated with the physiological phenotype of the groups of Sauropsids. The only exceptions that can be explained by ancestral pseudogenization events are *TFAM*, which was pseudogenized or not detected on the Serpent suborder, except in *Python bivittatus* (Figure 9), and *SQSTM1*, pseudogenized in the Emydidae family of the Testudines (Figure 10).

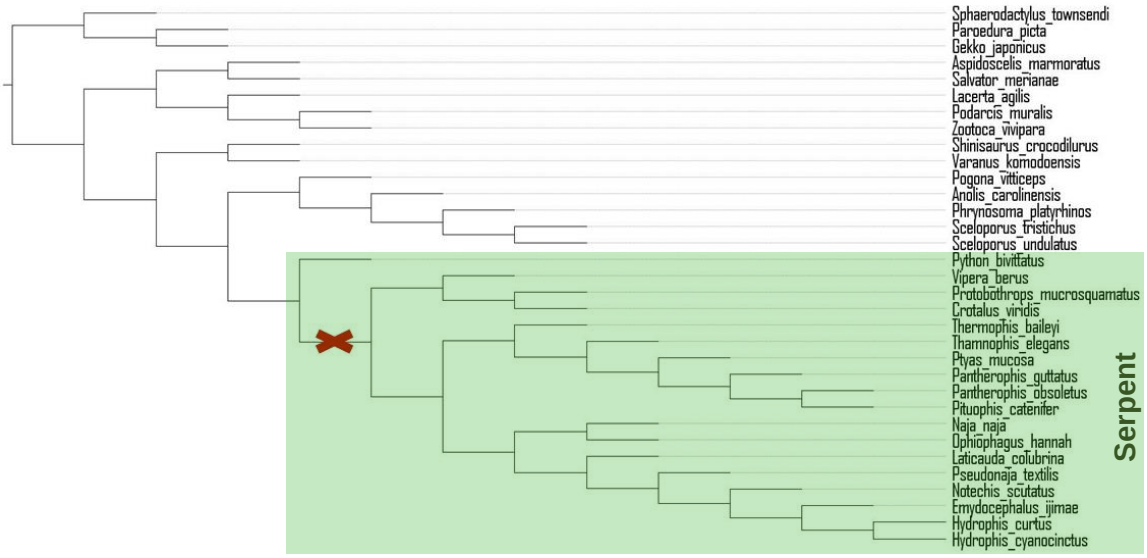

Figure 9 - Phylogeny of the Squamata showing the occurrence of TFAM pseudogenization, shared by the serpent species. This tree is based on the phylogeny shown is Figure 11.

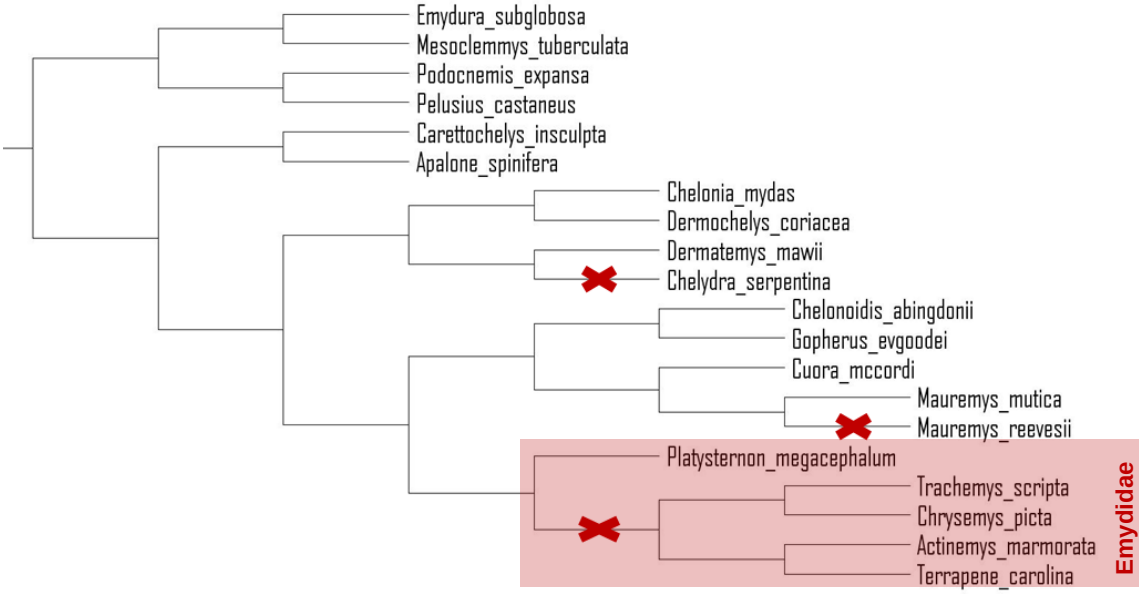

Figure 8 - Phylogeny of the Testudines showing the occurrence of the pseudogenization of the SQSTM1 in the Emydidae family. This tree is based on the phylogeny shown is Figure 11.

3.2. Model selection and partition analyses

The concatenated dataset was formed by the 72 genes that passed the quality control. The concatenated dataset was then subjected to nucleotide saturation analyses, presenting a Iss value significantly lower than the critical Iss value (Iss = 0.194; Iss.c = 0.400; *P*-value = 0.000).

For the whole dataset, GTR+I+G was computed as the best model of evolution, according to the corrected Akaike Information Criterion (AICc) (Table S9). The GARD analysis allowed the identification of 101 partitions in the concatenated dataset (Table S10).

3.3. Phylogeny

The phylogenetic reconstructions resulting from the partitioned and non-partitioned datasets were analysed and compared. Both phylogenies presented similar topologies and support values, maintaining the monophylies of all the avian and reptilian major clades and having successfully segregated every taxon. Therefore, considering the slightly higher bootstrap values of the partitioned tree, especially in the Tinamiformes clade, this phylogenetic reconstruction was used in the following analyses (Figure 11).

Figure 11 - Maximum-likelihood phylogenetic reconstruction, employing 72 genes associated with mitochondrial functions and considering 101 independent partitions. Only bootstraps values above 70 are shown.

3.4. Selection analyses

Most the synonymous substitution rate values for all assessed genes was below the recommended threshold (*dS* < 2) (Figure 12).

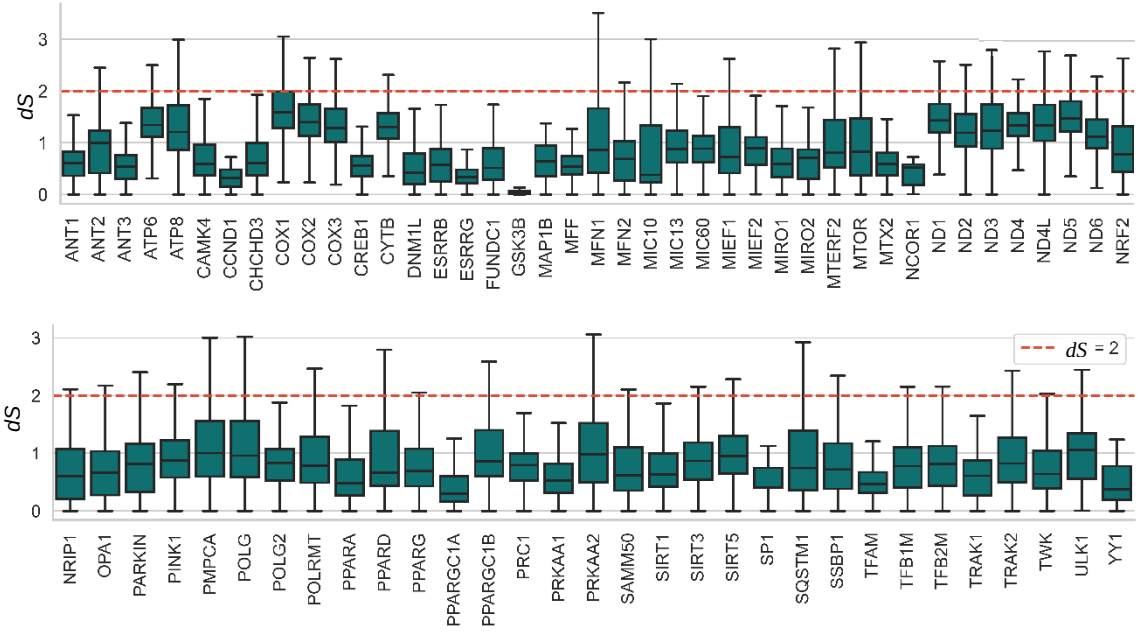

Figure 10 - Distribution of species synonymous substitution rates (*dS*) for each gene.

The branch site models revealed 5 genes with significant positive selection in birds, including 6 PSS (Figure 13A). While the genes *MIC13*, *PPARG* and *ULK1* are under positive selection within the avian clade, *ND1* and *ND5* showed evidence of positive selection in the avian ancestral branch, prior to the radiation of the extant bird lineages. Comparing the pattern of positive selection between the avian ancestral branch and the avian clade results, great variation is found. While for the ancestral branch the PSS occur in genes that participate in oxidative phosphorylation, for the avian clade three functions have genes under positive selection, the mitochondrial biogenesis, dynamics and mitophagy.

Additionally, there were found several genes under positive selection for Crocodylia and the Testudines clades. Contrary to the expectations, the Crocodylia lineage presented 6 genes subjected to positive selection, more than those found in birds (Figure 13B). On the other hand, Testudines presented 2 genes and Squamata displayed none (Figure 13C). Considering the Archosauria as a single group, composed of crocodiles and birds, three genes were subjected to positive selection (Figure 13D).

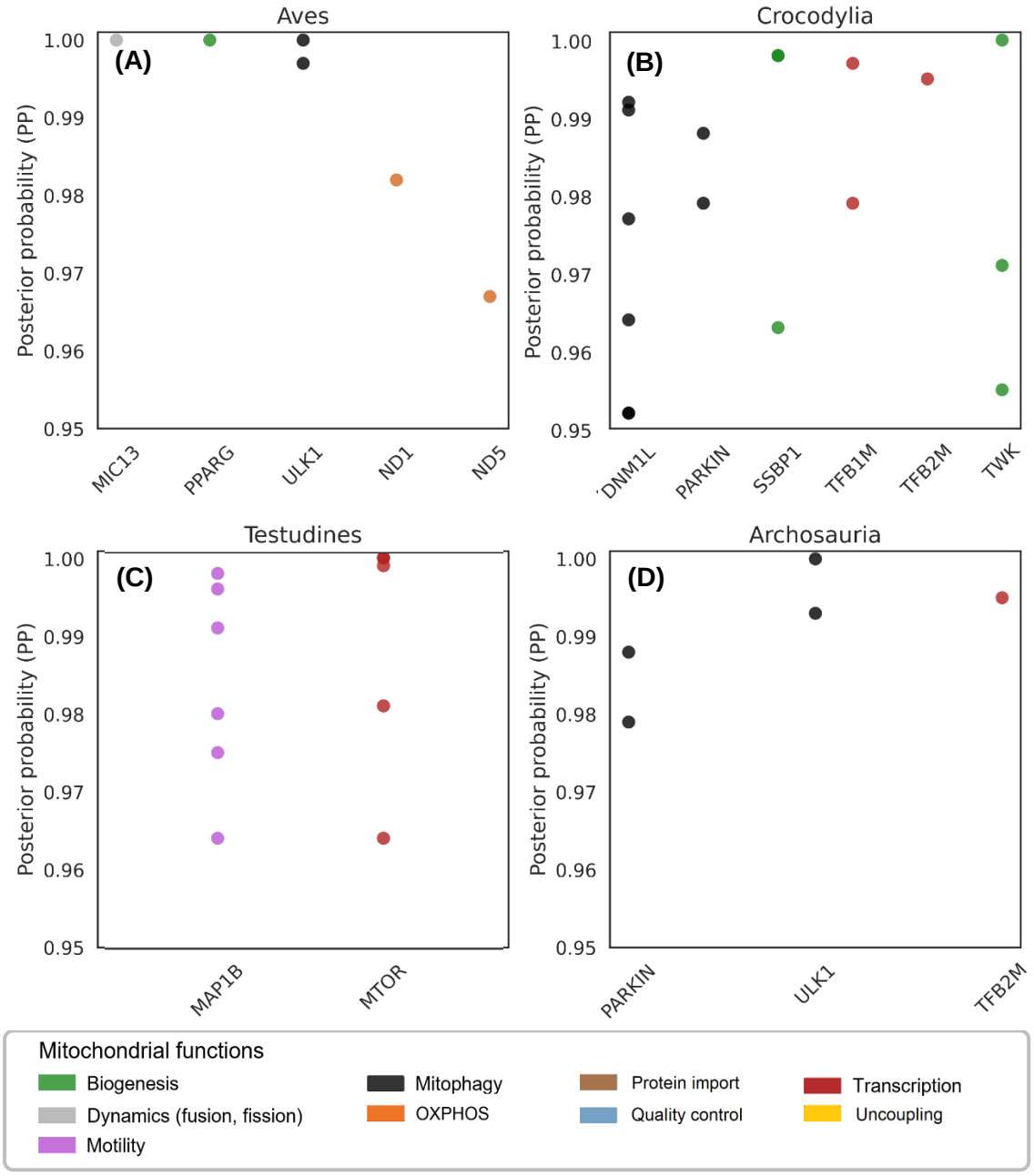

Figure 11 - Positively selected sites of the mitochondrial regulatory genes for birds and each of the reptile orders. Only were considered PSS that shown posterior probabilities superior to 0.95.

3.5. Evaluation of potential expression profiles

For the CAI, ENC, and Schi2 metrics, several genes were found to have significant higher codon usage bias in birds than in the reptile orders (Figure S2). It is important to remember that ENC corresponds to the absolute usage of a codon in a gene sequence, thus genes with higher CUB have lower ENC values. *MIEF1* presented a significantly higher CAI value (>0.8), which corresponds to a similarity of more than 80% of the codon composition of highly expressed ribosomal genes. Therefore, *MIEF1* should

also exhibit higher expression levels in birds than in reptiles. The other two gene-based metrics (ENC and Schi2) revealed the occurrence of higher codon usage bias in two avian genes (*PPARGC1B* and *PRKAA2*). Additionally, *DNM1L* also has higher codon usage bias in birds for the ENC metric. However, not all genes follow this pattern. While for CAI, none of the genes have higher values in reptiles, for both ENC and SChi2, there are two genes (*NRIP1* and *SIRT1*) with significantly higher values in reptiles than in birds (Figure S3).

For RSCU, a metric which provides values per codon, 26 genes had codons which were significantly more biased in avian species than in reptiles (Figure S4). Compared to the 41 biased codons for birds, only 2 codons with significantly higher bias were found in reptiles (Figure 14).

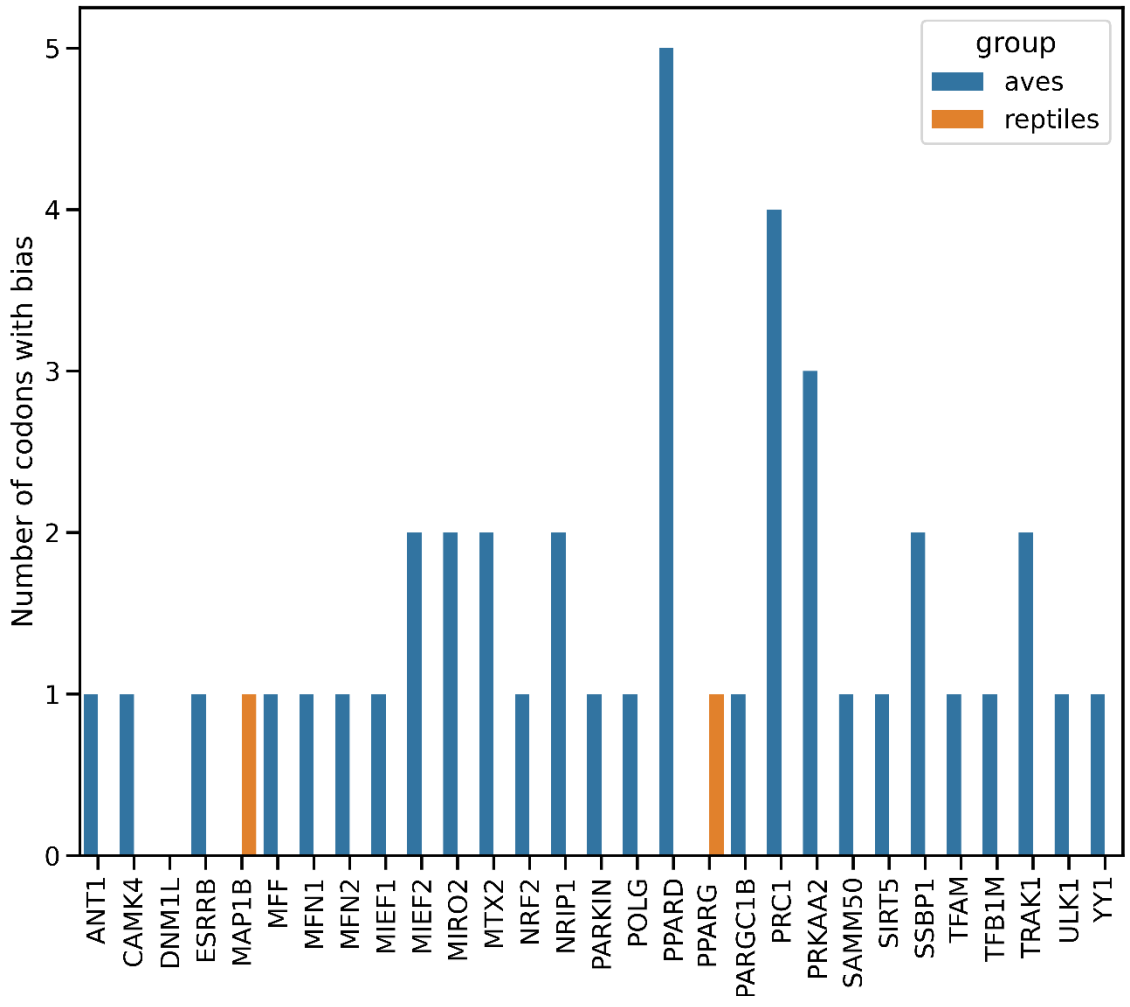

Figure 12 - Number of codons with significant biased in birds and reptiles for each gene.

Considering all the codon usage bias metrics used to evaluate the potential expression levels of the genes that regulate the mitochondrial functioning, there is a

small difference in the frequency of significantly biased genes of birds and reptiles for the three gene-based metrics. The higher bias of the bird genes is only perceptively larger when the codon-based metric (RSCU) is considered, with the number of genes with significantly higher codon usage bias being more than ten times larger in birds than reptiles (Figure 15).

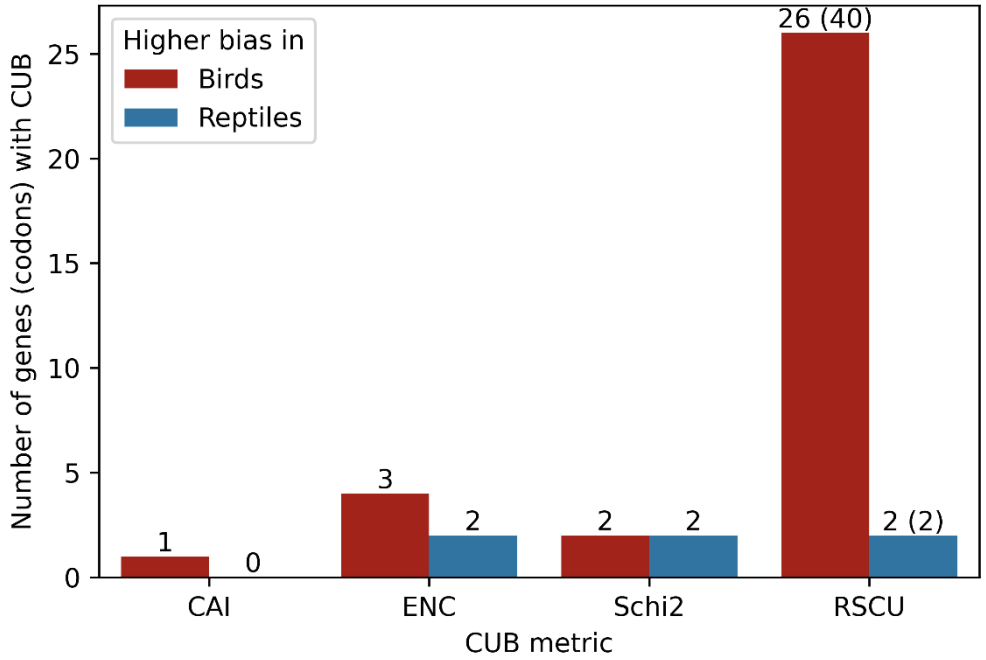

Figure 13 - Number of genes with significantly higher codon usage bias in birds and reptiles. For RSCU, the total number of codons with codon usage bias is represented between brackets above the bars.

However, if crocodiles and birds are considered as a single group, tested against the remaining reptiles, the differences remain (Figure 16). This way, the extant archosauria display more genes (and more codons) with CUB than turtles, lizards and snakes. For both ENC and Schi2 CCND1 and YY1 have higher codon usage bias in archosaurs than the other two reptile orders (Figure S5), while in Testudines and Squamata only TFAM is significantly more bias (Figure S6).

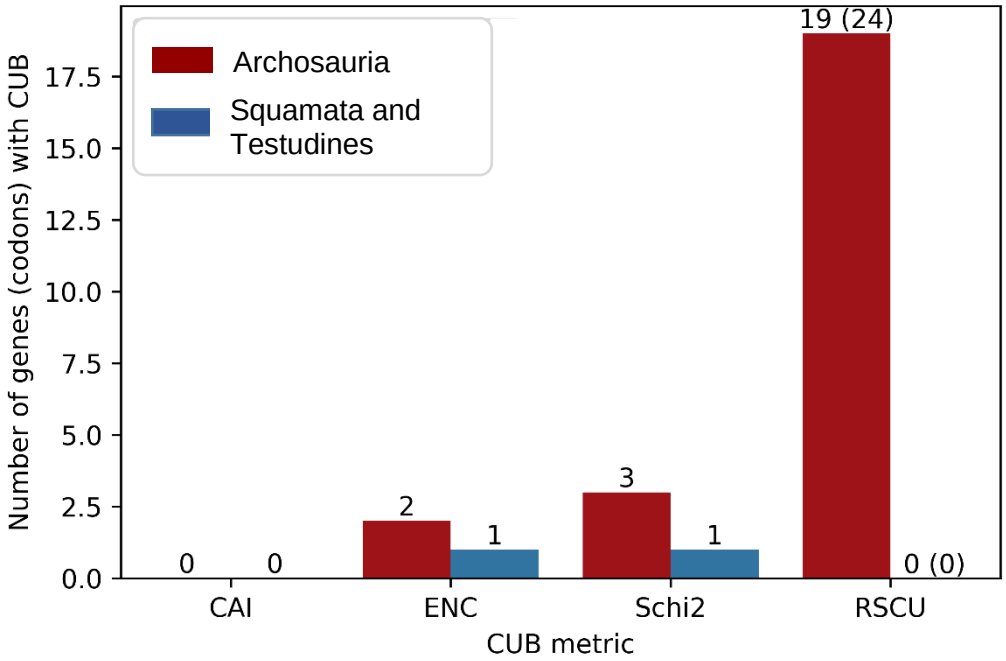

Figure 14 - Number of genes with significantly higher codon usage bias in Archosauria compared with the Squamata and Testudines. For RSCU the annotation above the bars depicts the total number of codons with codon usage bias between brackets.

3.6. Correlation

Correlation analyses were performed as an attempt to establish an association between the evolution of the genes that regulate the mitochondrial functions and several phenotype traits related to endothermy. Neither meaningful linear nor monotonic correlations between phenotypic and genetic traits were found for the concatenated dataset (Table S11). All the Pearson and Spearman correlations were negligible, with the highest value being a 0.181 correlation between the GC content and the mean body temperature. Still, several phenotype traits related with endothermy were correlated with each other (Figure 17). For example, there is a very high linear correlation between body temperature and the basal metabolic rate. On the other hand, the high non-linear correlation between the Enviromental temperature (Ta) and the latitude, was expected, because the temperatures tend to drop with the distance to the equator.

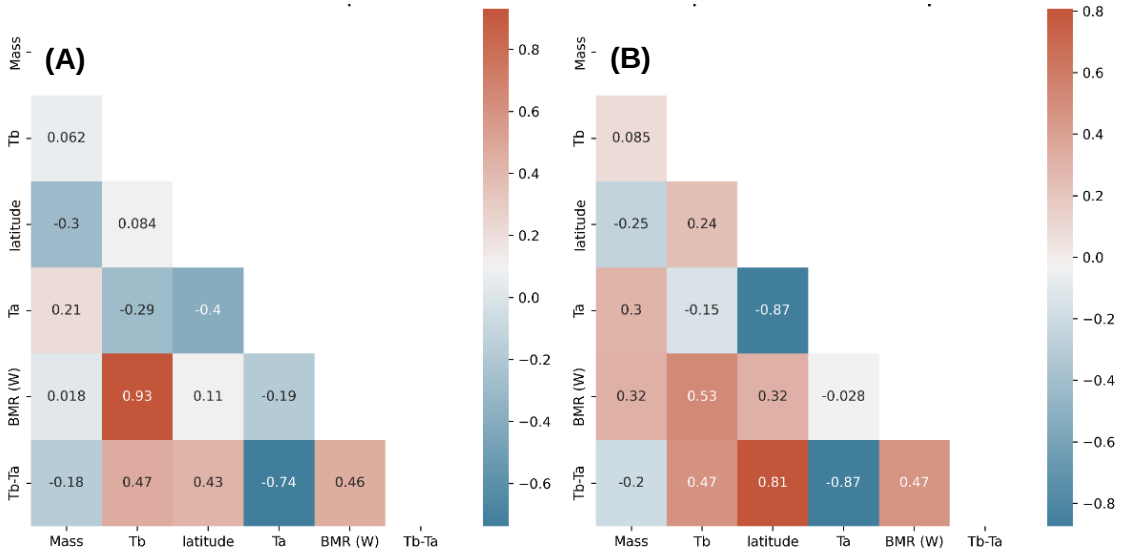

Figure 15 - Heatmaps of the Pearson (A) and Spearman (B) correlations between the phenotype traits related with endothermy. Mass = Body mass (g), Tb = Body temperature (ºC), latitude = distance to the equator, Ta = Environmental temperature (ºC), BMR = Basal metabolic rate (W), Tb-Ta = difference between the species average temperature and the average temperature of their centroid geographical distribution.

The lack of meaningful correlations was likely the result of non-informative genes, masking the results of informative genes. This way, by performing correlation tests considering each gene individually, the obtained results were pronounced. In these gene analyses, 37 significant high correlations were found, each with Pearson correlation coefficients (R) above 0.7 and based on information for more than 50 species (Figure S6).

In general, the correlations show that the mitochondrial regulatory genes of species with higher body temperatures, and consequently endotherms, tend to have higher GC contents, either generally or just at the 3rd codon position. These linear regression plots also reveal that endotherms usually have lower synonymous and non-synonymous substitution rates. The significant results of the correlations between body temperature and the codon usage bias metrics are less straightforward and present great variation from gene to gene. Both *POLG* and *PRKAA2* support that endotherms have higher codon usage bias in both metrics, as does *SP1* for the ENC metric. However, for other genes the correlations show the exact opposite, with MAP1B, MTX2, PARKIN and *SIRT1* showing that higher temperatures are associated with lower codon usage bias.

Besides the high correlations, there were also 112 moderate correlations (0.5 < R < 0.7). The distribution of all the significant correlations between phenotype traits and the genotype traits is illustrated in Figure 18.

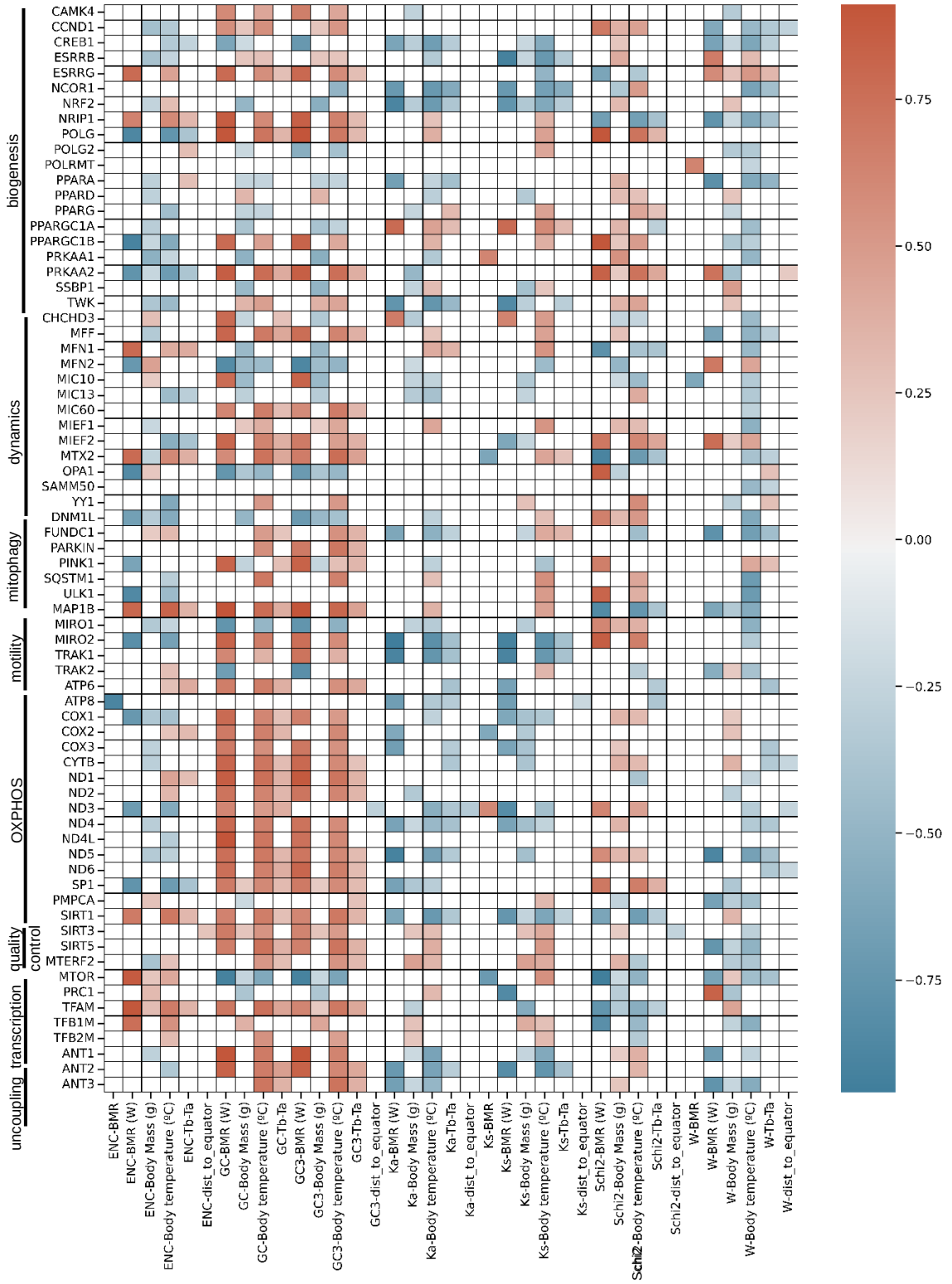

Figure 16 - Significant high (R>0.7) and moderate (0.5 < R < 0.7) correlations per gene.

The high correlations occur for 20 genes, representing all the functions except for mitochondrial protein import. These are all correlations between body temperature and 7 genotype traits (Figure S7). There are correlations with other phenotype factors, such as body mass and the difference of body temperature to the environmental temperature (Tb-Ta), but these are moderate ($0.5 < R < 0.7$) or low ($0.3 < R < 0.5$) (Figure 18). Should be referred that even though the standardize BMR metric did not return significant correlations, one of the initial metrics had some high correlations, but used less than 50 species to perform the correlations. Therefore, those correlations should be considered cautiously (Figure S8). For BMR there is more variation of patterns. Still, for most genes, species with higher basal metabolic rates and endotherms have genes with lower mutation rates and lower codon usage bias. There are only two genes which increase substitution rates towards higher BMR, *PPARGC1A* and *TWK*, while for codon usage bias only *MIRO2* has higher codon usage bias for higher BMR.

Discussion

The importance of the mitochondria on cellular bioenergetics and metabolism supports the hypothesis that these organelles have played a role in the increment of the metabolic rates [41, 43] and the acquisition of endothermy [43, 44]. Therefore, the higher mitochondrial density, efficiency, and membrane leakage, characteristic of endotherms, potentially resulted from molecular changes in the genes that code for the mitochondrial functions. It is yet unclear the exact time in which some Sauropsid lineages developed an endothermic profile [16, 17, 38]. The consensus is that endothermy evolved independently multiple times within the Sauropsids, in birds, and in some reptile lineages [14, 15, 17]. However, in recent years, there has been increasing support for the appearance of endothermy at the base of the Avemetatarsalia, the group formed by dinosaurs and birds, with a few of the dinosaur lineages subsequently having reversed to ectothermy [16, 17]. More recently, a study has provided detailed argumentation for a return to ectothermy in the crocodiles [17] and proposed that endothermy emerged before the divergence of birds and mammals, with reversions occurring later in reptile lineages [17]. However, no evidence of endothermy was found at the base of the Synapsids and instead, there has been detected a gradual transition to endothermy within this lineage [18]. To test each of these hypotheses, several genes with roles in the regulation of the mitochondrial function were selected and recovered from currently available bird and reptile genomes. These genes were then used in several analyses that allowed studying the differences between the four Sauropsid clades and assess

molecular changes behind the ectothermy-endothermy transition in the Sauropsid lineage.

The study of pseudogenization events can reveal much about the direction in which the selective pressures have acted [52]. However, no significant differences between Sauropsid orders were found in terms of frequency of non-functional sequences. The events of pseudogenisation occur mostly randomly and are not correlated with genome quality. Thus, the pseudogenizations seem to have no straightforward connection to the transition to endothermy and cannot be used in support for any of the mentioned evolutionary hypothesis. Only *TFAM* and *SQSTM1* have a phylogenetic pattern in their pseudogenization, which may indicate that these genes were subjected to neutral selection in those particular lineages [100].

Despite that, a mitochondrial role in the development of the endothermic profile is supported by the occurrence of adaptive molecular changes in birds' mitochondrial regulatory genes, either evidenced by positive selection and non-synonymous mutations, or higher codon usage bias and synonymous mutations, which can be used as a good proxy of the gene expression levels. Additionally, the high correlations obtained between the body temperatures and the basal metabolic rates also strengthen the support for a mitochondrial influence in the development and maintenance of endothermy. However, most of the genes that were found to be under positive selection in birds or reptiles do not have a high number of biased codons, indicating that, at least for the selected mitochondrial regulatory genes, the action of positive selection and synonymous codon selection might not be concurrent and, instead, act independently. This clearly indicates that not all mitochondrial regulatory genes are subjected to the same selective pressures and that they may exhibit a distinct degree of influence towards heat production and, ultimately, the origin of endothermy.

Nevertheless, the different analyses did not converge for the dichotomy of birds and reptiles, with a clear molecular separation between endotherms and ectotherms. It could be argued that the absence of clear dichotomy was caused by the separation of the reptile orders, which could have withered the endothermy molecular patterns, confounding them with order specific patterns. However, this hypothesis loses strength if the great diversity of the paraphyletic reptiles and the recent support for earlier origins are considered. Still there are five genes that support the importance of the mitochondria to endothermy and present significant evidence of positive selection in birds. Among these are three crucial genes: PPARG, ND1 and ND5. PPARG, similarly to PPARGC1A and PPARGC1B, is very important to mitochondrial regulation [101, 102], increasing and regulating most of mitochondrial functions, through influence on multiple mitochondrial

regulatory genes [101, 102]. On the other hand, ND1 and ND5 are crucial to ATP production, through their vital role on OXPHOS. Thus, the molecular changes of these genes in birds might have promoted the increases in metabolic rates and energy production that promoted the development of endothermy. Finding this significant differentiation between endotherms and ectotherms on such crucial genes suggests that positive selected sites found in these genes may have contributed to the overall mitochondrial and physiological changes that promoted endothermy's emergence. Still, a stronger support for the rise of endothermy at the base of the avian lineage comes from the codon usage bias analyses. In this analysis, birds display more genes with significantly higher codon usage bias, and potentially higher expression levels, than any of the reptile lineages. One of them, PPARGC1B, is especially relevant, due to its large influence on energy metabolism [102-104], resultant from its influence on several genes with roles on multiple mitochondrial regulatory functions [102-104]. An increase in the PPARGC1B codon usage bias would potentially means an increment of the gene expression levels, since synonymous codons have different transcriptional efficiencies. Therefore, a codon may be selected to allow faster transcription and translation, resulting in higher expression levels [82, 83, 105]. The increase in expression of PPARGC1B can then result in an enhancement of the mitochondrial functions and by consequence, an increase of the metabolism and energy production necessary to support endothermy [103]. Despite the fact that birds possess more codon biased genes, reptiles still show two genes with high codon usage bias. Interestingly, one of them, NRIP1, has been implicated in the regulation of mitochondrial biogenesis as a repressor in birds and mammals [106], acting as a brake to the mitochondrial biogenesis through interaction with other genes such as the ERR gene family and PPARs genes [107]. Assuming that its function remains conserved in reptiles, since NRIP1 leads to gene expression decreases for OXPHOS and biogenesis functions [107], the higher bias in reptiles could be related with their lower aerobic potential [108]. Therefore, this could be one of the molecular changes allowing their return to ectothermy. The other gene with higher codon usage bias in reptiles is SIRT1. Sirtuins (SIRTs) are implied on the mitochondrial quality control [109], through their roles in the reduction of oxidative stress through overexpression of antioxidant enzymes [109-111]. Nevertheless, SIRT1 can also lead to an improvement of mitochondrial function, through the increased expression of OXPHOS genes and mitochondrial biogenesis [109]. Considering that increased aerobic capacity, characteristic of endotherms, tends to lead to a higher production of reactive oxygen species (ROS) [112, 113], we should expect higher expression of SIRT1 in birds and, therefore, higher CUB. One possible explanation to the higher CUB found in reptiles,

could be that SIRT1 has a less significant role in birds, perhaps because mitochondrial quality control is more dependent on other genes, either one of the other sirtuins (SIRT3, SIRT4, SIRT5) or GSK3B.

Still, the absence of a clear ectotherm-endotherm transition and the positive selection found in the Crocodylia and Testudines may indicate an earlier rise of endothermy and a gradual transition to an endothermic profile. Thus, the global results seem to suggest an origin at the base of the Archosauria. Overall, an endothermic origin in the base of Archosaurs could help explain the high values of positive selection found in the Crocodiles. If we consider that an endothermic profile was developed earlier in the Archosauria, the crocodiles would have reverted to ectothermy [16, 17], perhaps as a result of the lower demand for high aerobic metabolism that their current ambush predatory strategies imply [17], they would be subjected to new selective pressures, which would consequently lead to the changes of the mitochondrial metabolism detected in this work. This hypothesis would also support the occurrence of selection in dinosaurs that has received increased support [16, 17]. According to Wiemann *et al.* (2022), several dinosaur groups, including theropods, the most closely related to modern birds, had significantly increased metabolic rates and potentially were already endothermic species [16]. Considering Archosauria as a single group, there are three genes under selection and two with high codon usage bias that are shared by birds and crocodiles, which could also support an origin before the divergence of crocodiles and birds.

Future additional analyses could complement those here performed to further assess the role of the mitochondrial regulatory genes and the mitochondrial function to the development of endothermy. A comparison of the codon usage bias results with transcriptomic data would help validate the results of these analyses and confirm if the mitochondrial regulatory genes have indeed higher expression levels in endotherms than in the ectotherms. Another strategy to assess the differences found in these genes between the two groups would be to consider the changes that occurred in the non-coding regulatory regions. Despite not being translated, these regions can have major impacts on the transcription of the genes and thus ultimately affect their expression levels [114-117]. The mutations and positive selected sites found for the bird and reptile genes could also be investigated to assess how impactful they were to the protein conformation, three-dimensional structure and functionality. Finally, a thoroughly comparison between the endothermy of birds and mammals could help elucidate if the physiology evolved independently in the two lineages, or if endothermy occurred early in the Amniotes, and thus is a plesiomorphic trait, only later lost in the reptiles.

Conclusion

The aerobic capacity model suggests endothermy evolved as a by-product of the metabolic rate increasement, consequence of selection for high levels of activity. Such changes would probably be influenced by functional improvement of the mitochondria efficiency, the energy use, and the refinement of the cell central metabolism. Thus, the increase of the metabolic rates, favouring endothermy, could have resulted from the mitochondrial changes found in endotherms. The increase of the mitochondrial efficiency and density, together with the increments of the mitochondrial membrane leakage would have enhanced the metabolic rates and allowed the development of increased energy and heat productions that would be behind endothermy. According to this hypothesis, it would be expected that genes that regulate the mitochondrial function would have an impact on the evolution of these mitochondrial changes and consequently on the rise of endothermy.

The generally high selective pressures, codon usage bias, and potentially gene expression levels in birds indicate that some of the molecular changes in the genes responsible for the regulation of mitochondria may have assisted the transition to endothermy. The role of the mitochondria to the rise of endothermy has only been reinforced by the find of significantly high correlations between the body temperature, basal metabolic rate, and the genetic factors of the genes that regulate the mitochondrial function. On the other hand, the initially unexpected high values found for crocodiles and the avian ancestors might be explained by some of the most recent hypotheses on endothermy and its evolution, which state that several dinosaur lineages would already be endotherms and argue for an ectothermy reversion in crocodiles.

References

1. Brusatte, S.L., J.K. O'Connor, and E.D. Jarvis, *The Origin and Diversification of Birds.* Curr Biol, 2015. **25**(19): p. R888-98.
2. Brusatte, Stephen L., Jingmai K. O'Connor, and Erich D. Jarvis, *The Origin and Diversification of Birds.* Current Biology, 2015. **25**(19): p. R888-R898.
3. Prum, R.O., et al., *A comprehensive phylogeny of birds (Aves) using targeted next-generation DNA sequencing.* Nature, 2015. **526**(7574): p. 569-573.
4. Töpfer, T., *Morphological Variation in Birds: Plasticity, Adaptation, and Speciation*, in *Bird Species: How They Arise, Modify and Vanish*, D.T. Tietze, Editor. 2018, Springer International Publishing: Cham. p. 63-74.
5. Brusatte, S.L., et al., *Gradual assembly of avian body plan culminated in rapid rates of evolution across the dinosaur-bird transition.* Curr Biol, 2014. **24**(20): p. 2386-92.
6. Pope, K.O., S.L. D'Hondt, and C.R. Marshall, *Meteorite impact and the mass extinction of species at the Cretaceous/Tertiary boundary.* Proceedings of the National Academy of Sciences, 1998. **95**(19): p. 11028-11029.
7. Brusatte, S.L., *Evolution: How Some Birds Survived When All Other Dinosaurs Died.* Current Biology, 2016. **26**(10): p. R415-R417.
8. Kuhl, H., et al., *An Unbiased Molecular Approach Using 3'-UTRs Resolves the Avian Family-Level Tree of Life.* Molecular Biology and Evolution, 2020.
9. Jarvis, E.D., et al., *Whole-genome analyses resolve early branches in the tree of life of modern birds.* Science (New York, N.Y.), 2014. **346**(6215): p. 1320-1331.
10. Nespolo, R.F., et al., *Using new tools to solve an old problem: the evolution of endothermy in vertebrates.* Trends in Ecology & Evolution, 2011. **26**(8): p. 414-423.
11. Price, E.R. and E.M. Dzialowski, *Development of endothermy in birds: patterns and mechanisms.* J Comp Physiol B, 2018. **188**(3): p. 373-391.
12. Block, B. and J. Finnerty, *Endothermy in fishes: a phylogenetic analysis of constraints, predispositions, and selection pressures.* Environmental Biology of Fishes, 2004. **40**: p. 283-302.
13. Dickson, K.A. and J.B. Graham, *Evolution and consequences of endothermy in fishes.* Physiol Biochem Zool, 2004. **77**(6): p. 998-1018.
14. Tattersall, G.J., et al., *Seasonal reproductive endothermy in tegu lizards.* Sci Adv, 2016. **2**(1): p. e1500951.

15. Brashears, J. and D.F. DeNardo, *Facultative thermogenesis during brooding is not the norm among pythons.* J Comp Physiol A Neuroethol Sens Neural Behav Physiol, 2015. **201**(8): p. 817-25.
16. Wiemann, J., et al., *Fossil biomolecules reveal an avian metabolism in the ancestral dinosaur.* Nature, 2022.
17. Grigg, G., et al., *Whole-body endothermy: ancient, homologous and widespread among the ancestors of mammals, birds and crocodylians.* Biol Rev Camb Philos Soc, 2022. **97**(2): p. 766-801.
18. KEMP, T.S., *The origin of mammalian endothermy: a paradigm for the evolution of complex biological structure.* Zoological Journal of the Linnean Society, 2006. **147**(4): p. 473-488.
19. Winslow, J., *Homeothermy*, in *Encyclopedia of Psychopharmacology*, I.P. Stolerman, Editor. 2010, Springer Berlin Heidelberg: Berlin, Heidelberg. p. 603-603.
20. Ivanov, K.P., *The development of the concepts of homeothermy and thermoregulation.* Journal of Thermal Biology, 2006. **31**(1): p. 24-29.
21. Gordon C. Grigg, Lyn A. Beard, and Michael L. Augee, *The Evolution of Endothermy and Its Diversity in Mammals and Birds.* Physiological and Biochemical Zoology, 2004. **77**(6): p. 982-997.
22. Hans O. Pörtner, *Climate Variability and the Energetic Pathways of Evolution: The Origin of Endothermy in Mammals and Birds.* Physiological and Biochemical Zoology, 2004. **77**(6): p. 959-981.
23. Hedrick, M.S. and S.S. Hillman, *What drove the evolution of endothermy?* J Exp Biol, 2016. **219**(Pt 3): p. 300-1.
24. McNab, B.K., *What determines the basal rate of metabolism?* J Exp Biol, 2019. **222**(Pt 15).
25. Hillman, S.S., et al., *Physiological vagility and its relationship to dispersal and neutral genetic heterogeneity in vertebrates.* The Journal of Experimental Biology, 2014. **217**(18): p. 3356-3364.
26. McCluskey, E.S., *TEMPERATURE REGULATION IN TETRAPOD VEREBRATES: ECTOTHERMS VS ENDOTHERMS.* 1982.
27. Mélanie, B., et al., *Allometry of mitochondrial efficiency is set by metabolic intensity.* Proc Biol Sci, 2019. **286**(1911): p. 20191693.
28. Bennett, A. and J. Ruben, *Endothermy and activity in vertebrates.* Science, 1979. **206**(4419): p. 649-654.

29. Hayes, J.P. and T. Garland, Jr., *THE EVOLUTION OF ENDOTHERMY: TESTING THE AEROBIC CAPACITY MODEL.* Evolution, 1995. **49**(5): p. 836-847.
30. Clarke, A. and H.O. Pörtner, *Temperature, metabolic power and the evolution of endothermy.* Biol Rev Camb Philos Soc, 2010. **85**(4): p. 703-27.
31. Koteja, P., *The evolution of concepts on the evolution of endothermy in birds and mammals.* Physiol Biochem Zool, 2004. **77**(6): p. 1043-50.
32. Nagy, K.A., I.A. Girard, and T.K. Brown, *Energetics of free-ranging mammals, reptiles, and birds.* Annu Rev Nutr, 1999. **19**: p. 247-77.
33. Lovegrove, B.G., *A phenology of the evolution of endothermy in birds and mammals.* Biol Rev Camb Philos Soc, 2017. **92**(2): p. 1213-1240.
34. Crompton, A., C.R. Taylor, and J.A. Jagger, *Evolution of homeothermy in mammals.* Nature, 1978. **272**(5651): p. 333-336.
35. McNab, B.K., *The evolution of endothermy in the phylogeny of mammals.* The American Naturalist, 1978. **112**(983): p. 1-21.
36. Farmer, C.G., *Parental Care: The Key to Understanding Endothermy and Other Convergent Features in Birds and Mammals.* Am Nat, 2000. **155**(3): p. 326-334.
37. Koteja, P., *Energy assimilation, parental care and the evolution of endothermy.* Proceedings of the Royal Society of London. Series B: Biological Sciences, 2000. **267**(1442): p. 479-484.
38. Rezende, E.L., et al., *Shrinking dinosaurs and the evolution of endothermy in birds.* Science Advances, 2020. **6**(1): p. eaaw4486.
39. Jastroch, M., et al., *Mitochondrial proton and electron leaks.* Essays Biochem, 2010. **47**: p. 53-67.
40. Klingenspor, M., *Cold-induced recruitment of brown adipose tissue thermogenesis.* Exp Physiol, 2003. **88**(1): p. 141-8.
41. Brand, M.D., *The contribution of the leak of protons across the mitochondrial inner membrane to standard metabolic rate.* Journal of Theoretical Biology, 1990. **145**(2): p. 267-286.
42. Moyes, C.D., *Controlling muscle mitochondrial content.* J Exp Biol, 2003. **206**(Pt 24): p. 4385-91.
43. Walter, I. and F. Seebacher, *Endothermy in birds: underlying molecular mechanisms.* J Exp Biol, 2009. **212**(Pt 15): p. 2328-36.
44. Else, P.L., *Mammals to membranes: A reductionist story.* Comp Biochem Physiol B Biochem Mol Biol, 2021. **253**: p. 110552.

45. Ashburner, M., et al., *Gene ontology: tool for the unification of biology. The Gene Ontology Consortium.* Nat Genet, 2000. **25**(1): p. 25-9.
46. *The Gene Ontology resource: enriching a GOld mine.* Nucleic Acids Res, 2021. **49**(D1): p. D325-d334.
47. Moreira, M.O., Y.-F. Qu, and J.J. Wiens, *Large-scale evolution of body temperatures in land vertebrates.* Evolution Letters, 2021. **5**(5): p. 484-494.
48. Benson, D.A., et al., *GenBank.* Nucleic Acids Res, 2013. **41**(Database issue): p. D36-42.
49. Consortium, T.U., *UniProt: the universal protein knowledgebase in 2021.* Nucleic Acids Research, 2020. **49**(D1): p. D480-D489.
50. Gertz, E.M., et al., *Composition-based statistics and translated nucleotide searches: improving the TBLASTN module of BLAST.* BMC biology, 2006. **4**: p. 41-41.
51. Slater, G.S.C. and E. Birney *Automated generation of heuristics for biological sequence comparison*. BMC bioinformatics, 2005. **6**, 31 DOI: 10.1186/1471-2105-6-31.
52. Li, W.-H., T. Gojobori, and M. Nei, *Pseudogenes as a paradigm of neutral evolution.* Nature, 1981. **292**(5820): p. 237-239.
53. Kumar, S., G. Stecher, and K. Tamura, *MEGA7: Molecular Evolutionary Genetics Analysis Version 7.0 for Bigger Datasets.* Mol Biol Evol, 2016. **33**(7): p. 1870-4.
54. Sela, I., et al., *GUIDANCE2: accurate detection of unreliable alignment regions accounting for the uncertainty of multiple parameters.* Nucleic Acids Research, 2015. **43**(W1): p. W7-W14.
55. Penn, O., et al., *An alignment confidence score capturing robustness to guide tree uncertainty.* Mol Biol Evol, 2010. **27**(8): p. 1759-67.
56. Kearse, M., et al., *Geneious Basic: an integrated and extendable desktop software platform for the organization and analysis of sequence data.* Bioinformatics, 2012. **28**(12): p. 1647-9.
57. Martinez-Gutierrez, C.A. and F.O. Aylward, *Phylogenetic Signal, Congruence, and Uncertainty across Bacteria and Archaea.* Molecular Biology and Evolution, 2021. **38**(12): p. 5514-5527.
58. Gadagkar, S.R., M.S. Rosenberg, and S. Kumar, *Inferring species phylogenies from multiple genes: concatenated sequence tree versus consensus gene tree.* J Exp Zool B Mol Dev Evol, 2005. **304**(1): p. 64-74.
59. Philippe, H., et al., *Resolving difficult phylogenetic questions: why more sequences are not enough.* PLoS biology, 2011. **9**(3): p. e1000602-e1000602.

60. Xia, X. and P. Lemey, *Assesing substitution saturation with DAMBE*. 2009. p. 611-626.
61. Xia, X., *DAMBE7: New and Improved Tools for Data Analysis in Molecular Biology and Evolution.* Mol Biol Evol, 2018. **35**(6): p. 1550-1552.
62. Shapiro, B., A. Rambaut, and A.J. Drummond, *Choosing Appropriate Substitution Models for the Phylogenetic Analysis of Protein-Coding Sequences.* Molecular Biology and Evolution, 2005. **23**(1): p. 7-9.
63. Bruno, W.J. and A.L. Halpern, *Topological bias and inconsistency of maximum likelihood using wrong models.* Mol Biol Evol, 1999. **16**(4): p. 564-6.
64. Posada, D., *The effect of branch length variation on the selection of models of molecular evolution.* J Mol Evol, 2001. **52**(5): p. 434-44.
65. Buckley, T.R. and C.W. Cunningham, *The Effects of Nucleotide Substitution Model Assumptions on Estimates of Nonparametric Bootstrap Support.* Molecular Biology and Evolution, 2002. **19**(4): p. 394-405.
66. Kainer, D. and R. Lanfear, *The Effects of Partitioning on Phylogenetic Inference.* Molecular Biology and Evolution, 2015. **32**(6): p. 1611-1627.
67. Lanfear, R., et al., *PartitionFinder: Combined Selection of Partitioning Schemes and Substitution Models for Phylogenetic Analyses.* Molecular Biology and Evolution, 2012. **29**(6): p. 1695-1701.
68. Frandsen, P.B., et al., *Automatic selection of partitioning schemes for phylogenetic analyses using iterative k-means clustering of site rates.* BMC Evolutionary Biology, 2015. **15**(1): p. 13.
69. Kosakovsky Pond, S.L., et al., *Automated Phylogenetic Detection of Recombination Using a Genetic Algorithm.* Molecular Biology and Evolution, 2006. **23**(10): p. 1891-1901.
70. Weaver, S., et al., *Datamonkey 2.0: A Modern Web Application for Characterizing Selective and Other Evolutionary Processes.* Molecular Biology and Evolution, 2018. **35**(3): p. 773-777.
71. Posada, D., *jModelTest: Phylogenetic Model Averaging.* Molecular Biology and Evolution, 2008. **25**(7): p. 1253-1256.
72. Minh, B.Q., et al., *IQ-TREE 2: New Models and Efficient Methods for Phylogenetic Inference in the Genomic Era.* Molecular Biology and Evolution, 2020. **37**(5): p. 1530-1534.
73. Rambaut, A., *FigTree, Version 1.4. 4*. 2018.
74. Rambaut, A. and A. Drummond, *FigTree version 1.4. 0*. 2012.

75. Darwin, C., *On the origin of species by means of natural selection, or the preservation of favoured races in the struggle for life*. 1859, London: John Murray.
76. Yang, Z., *PAML: a program package for phylogenetic analysis by maximum likelihood.* Bioinformatics, 1997. **13**(5): p. 555-556.
77. Yang, Z., *PAML 4: Phylogenetic Analysis by Maximum Likelihood.* Molecular Biology and Evolution, 2007. **24**(8): p. 1586-1591.
78. Maldonado, E., et al., *LMAP: Lightweight Multigene Analyses in PAML.* BMC Bioinformatics, 2016. **17**(1): p. 354.
79. Rozas, J., et al., *DnaSP 6: DNA Sequence Polymorphism Analysis of Large Data Sets.* Molecular Biology and Evolution, 2017. **34**(12): p. 3299-3302.
80. Aylward, F. *Introduction to calculating dN/dS ratios with codeml V.2*. 2018; Available from: https://www.protocols.io/view/introduction-to-calculating-dn-ds-ratios-with-code-3byl4o4rgo5d/v2.
81. Zhang, Z., et al., *Codon Deviation Coefficient: a novel measure for estimating codon usage bias and its statistical significance.* BMC Bioinformatics, 2012. **13**(1): p. 43.
82. Zhao, F., et al., *Genome-wide role of codon usage on transcription and identification of potential regulators.* Proceedings of the National Academy of Sciences, 2021. **118**(6): p. e2022590118.
83. Liu, Y., *A code within the genetic code: codon usage regulates co-translational protein folding.* Cell Communication and Signaling, 2020. **18**(1): p. 145.
84. Sharp, P.M., T.M. Tuohy, and K.R. Mosurski, *Codon usage in yeast: cluster analysis clearly differentiates highly and lowly expressed genes.* Nucleic acids research, 1986. **14**(13): p. 5125-5143.
85. Liu, S.S., et al., *A novel framework for evaluating the performance of codon usage bias metrics.* Journal of The Royal Society Interface, 2018. **15**(138): p. 20170667.
86. Petibon, C., et al., *Regulation of ribosomal protein genes: An ordered anarchy.* Wiley Interdiscip Rev RNA, 2021. **12**(3): p. e1632.
87. Subramanian, K., et al., *The Codon Statistics Database: a Database of Codon Usage Bias.* bioRxiv, 2022: p. 2022.03.29.486291.
88. Karlin, S. and J. Mrázek, *What Drives Codon Choices in Human Genes?* Journal of Molecular Biology, 1996. **262**(4): p. 459-472.
89. Galtier, N., et al., *Codon Usage Bias in Animals: Disentangling the Effects of Natural Selection, Effective Population Size, and GC-Biased Gene Conversion.* Molecular Biology and Evolution, 2018. **35**(5): p. 1092-1103.

90. Newman, Z.R., et al., *Differences in codon bias and GC content contribute to the balanced expression of TLR7 and TLR9.* Proceedings of the National Academy of Sciences, 2016. **113**(10): p. E1362-E1371.
91. Yakovchuk, P., E. Protozanova, and M.D. Frank-Kamenetskii, *Base-stacking and base-pairing contributions into thermal stability of the DNA double helix.* Nucleic Acids Res, 2006. **34**(2): p. 564-74.
92. Bernardi, G., *The neoselectionist theory of genome evolution.* Proc Natl Acad Sci U S A, 2007. **104**(20): p. 8385-90.
93. Xu, X.-z., et al., *Analysis of synonymous codon usage and evolution of begomoviruses.* Journal of Zhejiang University. Science. B, 2008. **9**(9): p. 667-674.
94. Naya, H., et al., *Translational selection shapes codon usage in the GC-rich genome of Chlamydomonas reinhardtii.* FEBS Letters, 2001. **501**(2): p. 127-130.
95. Puigbò, P., I.G. Bravo, and S. Garcia-Vallve, *CAIcal: A combined set of tools to assess codon usage adaptation.* Biology Direct, 2008. **3**(1): p. 38.
96. Sharp, P.M., et al., *Codon usage patterns in Escherichia coli, Bacillus subtilis, Saccharomyces cerevisiae, Schizosaccharomyces pombe, Drosophila melanogaster and Homo sapiens; a review of the considerable within-species diversity.* Nucleic Acids Res, 1988. **16**(17): p. 8207-11.
97. Lartillot, N. and R. Poujol, *A phylogenetic model for investigating correlated evolution of substitution rates and continuous phenotypic characters.* Mol Biol Evol, 2011. **28**(1): p. 729-44.
98. Andrade, C., *Z Scores, Standard Scores, and Composite Test Scores Explained.* Indian Journal of Psychological Medicine, 2021. **43**(6): p. 555-557.
99. Corp., I., *IBM SPSS Statistics for Windows, Version 27.0. Armonk, NY: IBM Corp.* 2020.
100. Kimura, M., *The Neutral Theory of Molecular Evolution*. 1983, Cambridge: Cambridge University Press.
101. Corona, J.C. and M.R. Duchen, *PPARγ as a therapeutic target to rescue mitochondrial function in neurological disease.* Free Radic Biol Med, 2016. **100**: p. 153-163.
102. Fan, W. and R. Evans, *PPARs and ERRs: molecular mediators of mitochondrial metabolism.* Current Opinion in Cell Biology, 2015. **33**: p. 49-54.
103. Cantó, C. and J. Auwerx, *PGC-1alpha, SIRT1 and AMPK, an energy sensing network that controls energy expenditure.* Curr Opin Lipidol, 2009. **20**(2): p. 98-105.

104. Ventura-Clapier, R., A. Garnier, and V. Veksler, *Transcriptional control of mitochondrial biogenesis: the central role of PGC-1alpha.* Cardiovasc Res, 2008. **79**(2): p. 208-17.
105. Xia, X., *Maximizing transcription efficiency causes codon usage bias.* Genetics, 1996. **144**(3): p. 1309-20.
106. Lin, J.D., *Minireview: the PGC-1 coactivator networks: chromatin-remodeling and mitochondrial energy metabolism.* Molecular endocrinology, 2009. **23**(1): p. 2-10.
107. Hock, M.B. and A. Kralli, *Transcriptional control of mitochondrial biogenesis and function.* Annu Rev Physiol, 2009. **71**: p. 177-203.
108. Gillooly, J.F., J.P. Gomez, and E.V. Mavrodiev, *A broad-scale comparison of aerobic activity levels in vertebrates: endotherms versus ectotherms.* Proceedings of the Royal Society B: Biological Sciences, 2017. **284**(1849): p. 20162328.
109. Kitada, M., et al., *Sirtuins and type 2 diabetes: role in inflammation, oxidative stress, and mitochondrial function.* Frontiers in endocrinology, 2019. **10**: p. 187.
110. Xu, J., M. Kitada, and D. Koya, *The impact of mitochondrial quality control by Sirtuins on the treatment of type 2 diabetes and diabetic kidney disease.* Biochimica et Biophysica Acta (BBA) - Molecular Basis of Disease, 2020. **1866**(6): p. 165756.
111. Ren, J., et al., *Characteristics of expression and regulation of sirtuins in chicken (Gallus gallus).* Genome, 2017. **60**(5): p. 431-440.
112. He, F., et al., *Redox Mechanism of Reactive Oxygen Species in Exercise.* Front Physiol, 2016. **7**: p. 486.
113. Buttemer, W.A., D. Abele, and D. Costantini, *From bivalves to birds: oxidative stress and longevity.* Functional Ecology, 2010. **24**(5): p. 971-983.
114. Li, Y., W. Shi, and W.W. Wasserman, *Genome-wide prediction of cis-regulatory regions using supervised deep learning methods.* BMC Bioinformatics, 2018. **19**(1): p. 202.
115. Cahill, J.A., et al., *Positive selection in noncoding genomic regions of vocal learning birds is associated with genes implicated in vocal learning and speech functions in humans.* Genome research, 2021. **31**(11): p. 2035-2049.
116. Cooper, *Regulation of Transcription in Eukaryotes*. 2nd edition ed. The Cell: A Molecular Approach. , ed. G.S.S. Associates. 2000.
117. Wang, X., et al., *Single nucleotide polymorphism in transcriptional regulatory regions and expression of environmentally responsive genes.* Toxicology and Applied Pharmacology, 2005. **207**(2, Supplement): p. 84-90.

118. Yoo, S.M. and Y.K. Jung, *A Molecular Approach to Mitophagy and Mitochondrial Dynamics.* Mol Cells, 2018. **41**(1): p. 18-26.
119. Yang, K., et al., *The Key Roles of GSK-3β in Regulating Mitochondrial Activity.* Cell Physiol Biochem, 2017. **44**(4): p. 1445-1459.
120. Dorn, G.W., 2nd, R.B. Vega, and D.P. Kelly, *Mitochondrial biogenesis and dynamics in the developing and diseased heart.* Genes & development, 2015. **29**(19): p. 1981-1991.
121. Kim, J., J.H. Lee, and V.R. Iyer, *Global identification of Myc target genes reveals its direct role in mitochondrial biogenesis and its E-box usage in vivo.* PLoS One, 2008. **3**(3): p. e1798.
122. Scarpulla, R.C., *Transcriptional paradigms in mammalian mitochondrial biogenesis and function.* Physiol Rev, 2008. **88**(2): p. 611-38.
123. Palikaras, K. and N. Tavernarakis, *Mitochondrial homeostasis: the interplay between mitophagy and mitochondrial biogenesis.* Exp Gerontol, 2014. **56**: p. 182-8.
124. Dominy, J.E. and P. Puigserver, *Mitochondrial biogenesis through activation of nuclear signaling proteins.* Cold Spring Harb Perspect Biol, 2013. **5**(7).
125. Scarpulla, R.C., *Nuclear control of respiratory gene expression in mammalian cells.* J Cell Biochem, 2006. **97**(4): p. 673-83.
126. Lima, T.I., et al., *Role of NCoR1 in mitochondrial function and energy metabolism.* Cell Biol Int, 2018. **42**(6): p. 734-741.
127. Privalsky, M.L. and M.L. Goodson, *Evolution of NCoR-1 and NCoR-2 corepressor alternative mRNA splicing in placental mammals.* BMC Res Notes, 2019. **12**(1): p. 343.
128. Twig, G., B. Hyde, and O.S. Shirihai, *Mitochondrial fusion, fission and autophagy as a quality control axis: the bioenergetic view.* Biochim Biophys Acta, 2008. **1777**(9): p. 1092-7.
129. Westermann, B., *Mitochondrial fusion and fission in cell life and death.* Nature Reviews Molecular Cell Biology, 2010. **11**(12): p. 872-884.
130. Chen, H. and D.C. Chan, *Physiological functions of mitochondrial fusion.* Ann N Y Acad Sci, 2010. **1201**: p. 21-5.
131. Wada, J. and A. Nakatsuka, *Mitochondrial Dynamics and Mitochondrial Dysfunction in Diabetes.* Acta Med Okayama, 2016. **70**(3): p. 151-8.
132. Whitaker, R., et al., *Mitochondrial Biogenesis as a Pharmacological Target: A New Approach to Acute and Chronic Diseases.* Annual review of pharmacology and toxicology, 2015. **56**.

133. Hoppins, S., *The regulation of mitochondrial dynamics.* Curr Opin Cell Biol, 2014. **29**: p. 46-52.
134. Carvalho, F., et al., *Listeria monocytogenes Exploits Mitochondrial Contact Site and Cristae Organizing System Complex Subunit Mic10 To Promote Mitochondrial Fragmentation and Cellular Infection.* mBio, 2020. **11**(1).
135. Varadi, A., et al., *Cytoplasmic dynein regulates the subcellular distribution of mitochondria by controlling the recruitment of the fission factor dynamin-related protein-1.* J Cell Sci, 2004. **117**(Pt 19): p. 4389-400.
136. Rizzuto, R., et al., *Close contacts with the endoplasmic reticulum as determinants of mitochondrial Ca2+ responses.* Science, 1998. **280**(5370): p. 1763-6.
137. Yi, M., D. Weaver, and G. Hajnóczky, *Control of mitochondrial motility and distribution by the calcium signal: a homeostatic circuit.* J Cell Biol, 2004. **167**(4): p. 661-72.
138. Yang, R.F., et al., *Suppression of Mic60 compromises mitochondrial transcription and oxidative phosphorylation.* Sci Rep, 2015. **5**: p. 7990.
139. Yang, R.F., et al., *Mitofilin regulates cytochrome c release during apoptosis by controlling mitochondrial cristae remodeling.* Biochem Biophys Res Commun, 2012. **428**(1): p. 93-8.
140. Xie, J., et al., *The mitochondrial inner membrane protein mitofilin exists as a complex with SAM50, metaxins 1 and 2, coiled-coil-helix coiled-coil-helix domain-containing protein 3 and 6 and DnaJC11.* FEBS Lett, 2007. **581**(18): p. 3545-9.
141. Armstrong, L.C., A.J. Saenz, and P. Bornstein, *Metaxin 1 interacts with metaxin 2, a novel related protein associated with the mammalian mitochondrial outer membrane.* J Cell Biochem, 1999. **74**(1): p. 11-22.
142. Luciano, P., et al., *Functional cooperation of the mitochondrial processing peptidase subunits.* J Mol Biol, 1997. **272**(2): p. 213-25.
143. Ashrafi, G. and T. Schwarz, *The pathways of mitophagy for quality control and clearance of mitochondria.* Cell Death & Differentiation, 2013. **20**(1): p. 31-42.
144. Picca, A., et al., *Mitochondrial quality control mechanisms as molecular targets in cardiac ageing.* Nature Reviews Cardiology, 2018. **15**(9): p. 543-554.
145. Torrens-Mas, M., et al., *Sirtuin 3 silencing impairs mitochondrial biogenesis and metabolism in colon cancer cells.* Am J Physiol Cell Physiol, 2019. **317**(2): p. C398-c404.
146. Di Rita, A., et al., *HUWE1 E3 ligase promotes PINK1/PARKIN-independent mitophagy by regulating AMBRA1 activation via IKKα.* Nature Communications, 2018. **9**(1): p. 3755.

147. Cardol, P., et al., *Chapter 13 - Oxidative Phosphorylation: Building Blocks and Related Components*, in *The Chlamydomonas Sourcebook (Second Edition)*, E.H. Harris, D.B. Stern, and G.B. Witman, Editors. 2009, Academic Press: London. p. 469-502.
148. Little, A.G., S.C. Lougheed, and C.D. Moyes, *Evolution of mitochondrial-encoded cytochrome oxidase subunits in endothermic fish: the importance of taxon-sampling in codon-based models.* Mol Phylogenet Evol, 2012. **63**(3): p. 679-84.
149. Kelly, D.P. and R.C. Scarpulla, *Transcriptional regulatory circuits controlling mitochondrial biogenesis and function.* Genes Dev, 2004. **18**(4): p. 357-68.
150. Scarpulla, R.C., *Nuclear activators and coactivators in mammalian mitochondrial biogenesis.* Biochim Biophys Acta, 2002. **1576**(1-2): p. 1-14.
151. Wu, Z., et al., *Mechanisms controlling mitochondrial biogenesis and respiration through the thermogenic coactivator PGC-1.* Cell, 1999. **98**(1): p. 115-24.
152. Demine, S., P. Renard, and T. Arnould, *Mitochondrial Uncoupling: A Key Controller of Biological Processes in Physiology and Diseases.* Cells, 2019. **8**(8).
153. Bround, M.J., D.M. Bers, and J.D. Molkentin, *A 20/20 view of ANT function in mitochondrial biology and necrotic cell death.* Journal of Molecular and Cellular Cardiology, 2020. **144**: p. A3-A13.
154. D. Lepage, J.W. *The Peters' Check-list of the Birds of the World (1931-1987) Database*. 2014 [cited 2022 05/2022]; Available from: https://avibase.bsc-eoc.org/peterschecklist.jsp.
155. Myhrvold, N.P., et al., *An amniote life-history database to perform comparative analyses with birds, mammals, and reptiles.* Ecology, 2015. **96**(11): p. 3109-3109.
156. de Magalhães, J.P. and J. Costa, *A database of vertebrate longevity records and their relation to other life-history traits.* J Evol Biol, 2009. **22**(8): p. 1770-4.
157. Meiri, S., *Traits of lizards of the world: Variation around a successful evolutionary design.* Global Ecology and Biogeography, 2018. **27**(10): p. 1168-1172.
158. McNab, B., *An Analysis of the Body Temperatures of Birds.* The Condor, 1966. **68**.
159. White, C.R., N.F. Phillips, and R.S. Seymour, *The scaling and temperature dependence of vertebrate metabolism.* Biology Letters, 2006. **2**(1): p. 125-127.
160. Wolfram|Alpha. 2022 18/06/2022]; Available from: https://www.wolframalpha.com/input/?i=climate+latitude+40.5%2C+longitude+-98.5.

161. McKechnie, A.E., R.P. Freckleton, and W. Jetz, *Phenotypic plasticity in the scaling of avian basal metabolic rate.* Proceedings of the Royal Society B: Biological Sciences, 2006. **273**(1589): p. 931-937.
162. IUCN. *The IUCN Red List of Threatened Species. Version 2021-3.* . 2021; Available from: https://www.iucnredlist.org.

Attachments

Table S1 - List of mitochondrial regulatory functions and the associated nuclear and mitochondrial genes. Mitochondrial genes are shown in bold.

Mitochondrial functions	**Description**	**Genes**	**References**
Mitochondrial biogenesis	Synthesis of new mitochondria [118]	CAMK4, CCND1, CHCHD3, CREB1, ESSRB, ESSRG, GSK3B, MTOR, MTX1, MTX2, MYC, NCOR1, NRF1, NRIP1, NFE2L2, PERM1, PPARA, PPARG, PPARGC1A, PPARGC1B, PRKAA1, PRKAA2, SAMM50, SSBP1	[107, 119-127]
Mitochondrial fission	Return to the common state by breaking the mitochondrial networks [128]. Results in more diverse and fragmented mitochondria with small spherical shapes [129], displaying more variable energetic power and metabolic activities [124, 129, 130]].	DRP1, FIS1, GSK3B, MFF, MIC10, MIEF1, MIEF2, OPA1, PPARGC1A	[124, 131-134]
Mitochondrial fusion	Two mitochondria fuse, forming tubular and elongated interconnected	FIS1, GSK3B, MFN, MFN2, OPA1, PPARGC1A, PARKIN	

	mitochondria [135, 136], called mitochondrial networks, which result in genetic and biochemical homogeneity, by mixing the fused mitochondria content [128] and are essential to guarantee the higher energetic power and metabolism [130]		
Mitochondrial motility	Movement of the mitochondria to the location in the cell where their ATP production is demanded [124, 137]	GSK3B, MAP1B, MIC60, MIRO1, MIRO2, TRAK1, TRAK2	[107, 119, 138, 139]
Mitochondrial protein import	Escort and import of proteins of nuclear encoded genes necessary to mitochondrial function [104, 124]	CHCHD3, MTX1, MTX2, PMPCA, PPARGC1A, SAMM50	[140-142]
Mitochondrial quality control	Guarantees the maintenance of healthy mitochondrial mass [118, 124, 143] and mitochondrial homeostasis [144]	GSK3B, SIRT1, SIRT3, SIRT4, SIRT5	[124, 145]

Mitochondrial transcription	Transcription of the mitochondrial DNA [104]	MTERF, POLG, POLG2, POLRMT, TFAM, TFB1M, TFB2M, TWNK, YY1	[107, 121, 122, 124, 125]
Mitophagy	Elimination of damaged mitochondria [118]	FIS1, FUNDC1, MFN1, MFN2, PARIS, PARKIN, PINK1, SQSTM1	[107, 119, 124, 146]
Oxidative phosphorylation	Electron transfer chain coupled to the synthesis of ATP through a electrochemical transmembrane gradient [147]	**ATP6**, **ATP8**, NCOR1, **ND1**, **ND2**, **ND3**, **ND4**, **ND4L**, **ND5**, **ND6**, **CO1**, **CO2**, **CO3**, **CYTB**, GSK3B, MFF, NRF1, NFE2L2, PRKAA1, PRKAA2, SAMM50, TFAM, SP1, YY1	[43, 104, 107, 119, 148-151]
Mitochondrial uncoupling	Disruption of mitochondrial coupling through leakage of protons back through the membrane. Proton leak increases oxygen consumption and energy will be dissipated as heat instead of leading to the formation of ATP.	ANT1, ANT2, ANT3	[152, 153]

Table S2 - List of genomes from bird species used in the present study.

Species	Order	Accession number
Anas platyrhynchos	Anseriformes	VSDN00000000.1
Anas zonorhyncha	Anseriformes	NOIK00000000.1
Anser brachyrhynchus	Anseriformes	NXHY00000000.1
Anser cygnoides	Anseriformes	WTSS00000000.1
Anser indicus	Anseriformes	VDDG00000000.1
Anseranas semipalmata	Anseriformes	VXAA00000000.1
Asarcornis scutulata	Anseriformes	VZSO00000000.1
Aythya fuligula	Anseriformes	WNMM00000000.1
Branta canadensis	Anseriformes	SNRU00000000.1
Cairina moschata	Anseriformes	QZEJ00000000.1
Chauna torquata	Anseriformes	VXAL00000000.1
Cygnus atratus	Anseriformes	JABXOC000000000.1
Cygnus cygnus	Anseriformes	BMBB00000000.1
Cygnus olor	Anseriformes	WNMI00000000.1
Heteronetta atricapilla	Anseriformes	JAACYQ000000000.1
Nettapus auritus	Anseriformes	JAACYP000000000.1
Oxyura jamaicensis	Anseriformes	JAACYN000000000.1
Stictonetta naevosa	Anseriformes	JAACYO000000000.1
Apteryx haastii	Apterygiformes	PTFD00000000.1
Apteryx owenii	Apterygiformes	PTFC00000000.1
Apteryx rowi	Apterygiformes	PTFB00000000.1
Casuarius casuarius	Casuariiformes	PTFA00000000.1
Dromaius novaehollandiae	Casuariiformes	JABVCD000000000.1
Anomalopteryx didiformis	Dinornithiformes	SZQC00000000.1
Alectura lathami	Galliformes	VXAV00000000.1
Bambusicola thoracicus	Galliformes	PPHD00000000.1
Callipepla squamata	Galliformes	MCFN00000000.1
Chrysolophus pictus	Galliformes	JRFT00000000.1
Colinus virginianus	Galliformes	AWGT00000000.2
Coturnix japonica	Galliformes	LSZS00000000.1
Gallus gallus	Galliformes	JAENSK000000000.1
Lagopus muta	Galliformes	BJCA00000000.1
Lyrurus tetrix	Galliformes	JDSL00000000.1

Meleagris gallopavo	Galliformes	ADDD00000000.2
Numida meleagris	Galliformes	JABXER000000000.1
Odontophorus gujanensis	Galliformes	VXAB00000000.1
Pavo cristatus	Galliformes	QZWQ00000000.1
Pavo muticus	Galliformes	JACDJE000000000.1
Penelope pileata	Galliformes	WBMW00000000.1
Phasianus colchicus	Galliformes	WUCP00000000.1
Syrmaticus mikado	Galliformes	QGNR00000000.1
Tympanuchus cupido	Galliformes	MOXI00000000.1
Rhea americana	Rheiformes	PTJI00000000.1
Rhea pennata	Rheiformes	PTEV00000000.1
Struthio camelus	Struthioniformes	JJRT00000000.1
Crypturellus cinnamomeus	Tinamiformes	PTEZ00000000.1
Crypturellus soui	Tinamiformes	VWPX00000000.1
Crypturellus undulatus	Tinamiformes	VWPW00000000.1
Eudromia elegans	Tinamiformes	PTEX00000000.1
Nothocercus julius	Tinamiformes	VZSV00000000.1
Nothocercus nigrocapillus	Tinamiformes	WBNA00000000.1
Nothoprocta ornata	Tinamiformes	VZSH00000000.1
Nothoprocta pentlandii	Tinamiformes	VZSG00000000.1
Nothoprocta perdicaria	Tinamiformes	PTEW00000000.1
Tinamus guttatus	Tinamiformes	JMFW00000000.2

Table S3 - List of genomes from reptile species used in the present study.

Species	**Order**	**Accession number**
Alligator mississippiensis	Crocodylia	AKHW00000000.3
Alligator sinensis	Crocodylia	AVPB00000000.1
Crocodylus porosus	Crocodylia	MDVP00000000.1
Gavialis gangeticus	Crocodylia	MDVQ00000000.1
Sphenodon punctatus	Rhynchocephalia	QEPC00000000.1
Anolis carolinensis	Squamata	AAWZ00000000.2
Aspidoscelis marmoratus	Squamata	MTQE00000000.1
Crotalus viridis	Squamata	PDHV00000000.2
Emydocephalus ijimae	Squamata	BHEV00000000.1
Gekko japonicus	Squamata	LNDG00000000.1

Hydrophis curtus	Squamata	JABAHG000000000.1
Hydrophis cyanocinctus	Squamata	JAAZTL000000000.1
Lacerta agilis	Squamata	WNMS00000000.1
Laticauda colubrina	Squamata	BLBF00000000.1
Naja naja	Squamata	SOZL00000000.1
Notechis scutatus	Squamata	ULFQ00000000.1
Ophiophagus hannah	Squamata	AZIM00000000.1
Pantherophis guttatus	Squamata	JTLQ00000000.2
Pantherophis obsoletus	Squamata	WJSR00000000.1
Paroedura picta	Squamata	BDOT00000000.2
Phrynosoma platyrhinos	Squamata	JAIPUX000000000.1
Pituophis catenifer	Squamata	JAHUAB000000000.1
Podarcis muralis	Squamata	SIRZ00000000.1
Pogona vitticeps	Squamata	CEMB00000000.1
Protobothrops mucrosquamatus	Squamata	BCNE00000000.2
Pseudonaja textilis	Squamata	ULFR00000000.1
Ptyas mucosa	Squamata	WNWU00000000.1
Python bivittatus	Squamata	AEQU00000000.2
Salvator merianae	Squamata	QVOM00000000.2
Sceloporus tristichus	Squamata	JACSCI000000000.1
Sceloporus undulatus	Squamata	JAGXEY000000000.1
Shinisaurus crocodilurus	Squamata	JAHFWL000000000.1
Sphaerodactylus townsendi	Squamata	JAHVXK000000000.1
Thamnophis elegans	Squamata	WNNA00000000.1
Thermophis baileyi	Squamata	QLTV00000000.1
Varanus komodoensis	Squamata	SJPD00000000.1
Vipera berus	Squamata	JTGP00000000.1
Zootoca vivipara	Squamata	JAATIO000000000.1
Actinemys marmorata	Testudines	VOGN00000000.1
Apalone spinifera	Testudines	APJP00000000.1
Carettochelys insculpta	Testudines	VOCQ00000000.1
Chelonia mydas	Testudines	JADCQM000000000.2
Chelonoidis abingdonii	Testudines	PKMU00000000.1
Chelydra serpentina	Testudines	JAHGAV000000000.1
Chrysemys picta	Testudines	AHGY00000000.3

Cuora mccordi	Testudines	RQSS00000000.1
Dermatemys mawii	Testudines	VOCN00000000.1
Dermochelys coriacea	Testudines	WSPL00000000.4
Emydura subglobosa	Testudines	VOCO00000000.1
Gopherus evgoodei	Testudines	VHHN00000000.1
Mauremys mutica	Testudines	JAHDVG000000000.1
Mauremys reevesii	Testudines	JADWOL000000000.1
Mesoclemmys tuberculata	Testudines	VOCS00000000.1
Pelodiscus sinensis	Testudines	AGCU00000000.1
Pelusios castaneus	Testudines	VOCT00000000.1
Platysternon megacephalum	Testudines	QXTE00000000.1
Podocnemis expansa	Testudines	VOCP00000000.1
Terrapene carolina	Testudines	PRFB00000000.2
Trachemys scripta	Testudines	VIRI00000000.1

Table S4 - Queries used in the gene extraction for each gene in birds.

Gene	**Aves**	
ANT1	*G.gallus*	Q5ZMJ6
ANT2	*G.gallus*	A0A1D5PCU1
ANT3	*G.gallus*	Q5ZLG7
ATP6	*G.gallus*	P14092
ATP8	*G.gallus*	P14093
CAMK4	*G.gallus*	A0A1L1RWI9
CCND1	*G.gallus*	P55169
CHCHD3	*G.gallus*	A0A1L1RNV8
COX1	*G.gallus*	P18943
COX2	*G.gallus*	P18944
COX3	*G.gallus*	P18945
CREB1	*G.gallus*	Q7SX83
CYTB	*G.gallus*	P18946
DNM1L	*G.gallus*	A0A3Q2UHM4
ESRRB	*G.gallus*	A0A1D5NVI7
ESRRG	*G.gallus*	A0A1D5PH30
FUNDC1	*G.gallus*	E1BWM5
GSK3B	*G.gallus*	A0A3Q2TVV5

MAP1B	*G.gallus*	E1C1Q2
MFF	*G.gallus*	E1C541
MFN1	*G.gallus*	A0A1D5PYU0
MFN2	*G.gallus*	E1BSH7
MIC10	*G.gallus*	F1NWZ5
MIC13	*G.gallus*	A0A3Q2U8C2
MIC60	*G.gallus*	A0A3Q3AHD7
MIEF1	*G.gallus*	E1BVG4
MIEF2	*G.gallus*	F1P228
MIRO1	*G.gallus*	Q5ZM73
MIRO2	*G.gallus*	Q5ZM83
MTERF2	*G.gallus*	F1NYE8
MTOR	*G.gallus*	F1NUX4
MTX1	*A. fuligula*	A0A6J3EB23
MTX2	*G.gallus*	E1BVN1
MYC	*G.gallus*	P01109
NCOR1	*A. semipalmata*	A0A7K9UWB7
ND1	*G.gallus*	P18936
ND2	*G.gallus*	O63796
ND3	*G.gallus*	P18938
ND4	*G.gallus*	P18939
ND4L	*G.gallus*	P18942
ND5	*G.gallus*	P18940
ND6	*G.gallus*	Q06059
NRF1	*G.gallus*	Q5ZL67
NRF2	*A. platyrhynchos*	A0A493TEC3
NRIP1	*G.gallus*	R4GIS3
OPA1	*G.gallus*	Q5F499
PARKIN	*G.gallus*	A0A3Q2U9L6
PERM1	*G.gallus*	A0A1L1RV84
PINK1	*A. platyrhynchos*	U3IJA2
POLG	*G.gallus*	A0A1L1RT70
POLG2	*G.gallus*	F1NM24
POLRMT	*G.gallus*	E1BZ13
PMPCA	*G.gallus*	Q5ZJ49
PPARA	*G.gallus*	A0A1D5PJQ2
PPARD	*G.gallus*	A0A3Q3AXA2
PPARG	*G.gallus*	A0A3Q3ACW5
PPARGC1A	*G.gallus*	A0A1D5PN42

PPARGC1B	*A. platyrhynchos*	A0A493T1H1
PRC1	*G.gallus*	F1P2A8
PRKAA1	*G.gallus*	Q2PUH1
PRKAA2	*G.gallus*	Q2LAI0
SAMM50	*G.gallus*	E1C8A2
SIRT1	*G.gallus*	F1N886
SIRT3	*G.gallus*	A0A1D5NYI2
SIRT4	*G.gallus*	F1NB70
SIRT5	*G.gallus*	E1BRE2
SSBP1	*G.gallus*	E1BTE0
SP1	*G.gallus*	A0A1D5PXV5
SQSTM1	*G.gallus*	A0A1D5PLN4
TFAM	*G.gallus*	F1NG46
TFB1M	*G.gallus*	E1BWX0
TFB2M	*G.gallus*	F1NSS3
TRAK1	*G.gallus*	A0A3Q2U6F6
TRAK2	*G.gallus*	F1NVL2
TWNK	*G.gallus*	Q5ZIW1
ULK1	*G.gallus*	F1NZ50
YY1	*G.gallus*	F1NHV6

Table S5 - Queries used in the gene extraction for each gene and reptile order.

Gene	**Crocodylia**		**Squamata**		**Testudines**	
ANT1	XP_019377459.1	*G.gangeticus*	XP_020658275.1	*P.vitticeps*	XP_007068661	*C.mydas*
ANT2	XP_019395770.1	*C.porosus*	XP_032993345.1	*L.agilis*	XP_037764551.1	*C.mydas*
ANT3	XP_019384943.1	*C. porosus*	XP_033003375.1	*L. agilis*	XP_037755423.1	*C. mydas*
ATP6	O47872	*A.mississippiensis*	O79551	*Lycodon semicarinatus*	O79675	*Pelomedusa subrufa*
ATP8	O47871	*A. mississippiensis*	O79550	*Lycodon semicarinatus*	O79674	*P. subrufa*
CAMK4	XP_019388018.1	*C.porosus*	XP_028603715.1	*P. murallis*	XP_037757463.1	*C. mydas*
CCND1	XP_019407210.1	*C. porosus*	XP_020638518.1	*P.vitticeps*	XP_007068004.1	*C. mydas*

CHCHD3	XP_019399311.1	*C. porosus*	XP_033017350.1	*L. agilis*	XP_037745299.1	*C. mydas*
COX1	YP_637142.1	*C. porosus*	O79548	*L.semicarinatus*	O79672	*P. subrufa*
COX2	O47870	*A.mississippiensis*	O79549	*L.semicarinatus*	O79673	*P. subrufa*
COX3	YP_637146.1	*C.porosus*	O79552	*L.semicarinatus*	O79676	*P. subrufa*
CREB1	XP_019409597.1	*C. porosus*	XP_033026105.1	*L. agilis*	XP_007071892.2	*C.mydas*
CYTB	*YP_637152.1*	*C. porosus*	*B3GT02*	*A.carolinensis*	YP_009944895.1	-
DNM1L	*XP_019400186.1*	*C. porosus*	*G1KMD1*	*A.carolinensis*	XP_037734645.1	-
ESRRB	XP_019407648.1	*C. porosus*	XP_028574929.1	*P. murallis*	XP_044868535.1	*M.mutica*
ESRRG	XP_019405019.1	*C.porosus*	XP_028580475.1	*P. murallis*	XP_043399587.1	*C. mydas*
FUNDC1	XP_019384601.1	*C. porosus*	A0A803TNZ4	*A.carolinensis*	XP_037758722.1	*C. mydas*
GSK3B	XP_019404260.1	*C. porosus*	H9G7Y1	*A.carolinensis*	XP_037765566.1	*C. mydas*
MAP1B	XP_019387825.1	*C.porosus*	XP_020645886.1	*P.vitticeps*	XP_043403691.1	*C. mydas*
MFF	XP_019388576.1	*C.porosus*	G1KCL4	*A.carolinensis*	XP_027673153.1	*C. mydas*
MFN1	XP_019388304.1	*C.porosus*	G1KD85	*A.carolinensis*	XP_039344070.1	*M.reevesii*
MFN2	XP_019349522.1	*A.mississippiensis*	XP_020637811.1	*P.vitticeps*	XP_043387498.1	*C. mydas*
MIC10	XP_019397043.1	*C. porosus*	XP_033015326.1	*L. agilis*	XP_037736988.1	*C.mydas*
MIC13	XP_019406114.1	*C.porosus*	XP_020649863.1	*P. vitticeps*	XP_037741368.1	*C. mydas*
MIC60	XP_019408205.1	*C. porosus*	G1KLN0	*A.carolinensis*	XP_037754206.1	*C. mydas*
MIEF1	XP_019400504.1	*C. porosus*	A0A803TFR7	*A.carolinensis*	XP_039353044.1	*C.mydas*
MIEF2	XP_019397473.1	*C. porosus*	XP_016853379.1	*A.carolinensis*	XP_043380194.1	*C.mydas*
MIRO1	XP_025052095.1	*A.sinensis*	XP_020639216.1	*P.vitticeps*	XP_037769422.1	*C. mydas*

MIRO2	XP_014375631.1	*A.sinensis*	XP_033022757.1	*L.agilis*	XP_037766456.1	*C. mydas*
MTERF2	XP_019400339.1	*C. porosus*	G1KQX1	*A. carolinensis*	XP_043398258.1	*C.mydas*
MTOR	XP_019397229.1	*C. porosus*	XP_020637828.1	*P.vitticeps*	XP_037737122.1	*C.mydas*
MTX1	XP_019412275.1	*C.porosus*	XP_020653121.1	*P.vitticeps*	XP_037739590.1	*C.mydas*
MTX2	XP_019409795.1	*C. porosus*	H9GBJ9	*A. carolinensis*	XP_037768086.1	*C. mydas*
MYC	-	-	XP_033011747.1	*L. agilis*	XP_034619507.1	*T.scripta*
NCOR1	XP_019401306.1	*C. porosus*	XP_020664714.1	*P.vitticeps*	XP_043387092.1	*C. mydas*
ND1	O47868	*A. mississippiensis*	Q94YT7	*Varanus dumerilii*	O79670	*P. subrufa*
ND2	YP_637141.1	*C. porosus*	Q94VJ9	*Varanus baritji*	O79671	*P. subrufa*
ND3	O47874	*A.mississippiensis*	O79553	*L.semicarinatus*	NP_008771.1	*C. mydas*
ND4	YP_637149.1	*C.porosus*	B3GSZ9	*A. carolinensis*	O79677	*P.subrufa*
ND4L	YP_637148.1	*C. porosus*	O79554	*L.semicarinatus*	YP_005088194.1	*M. sinensis*
ND5	YP_637150.1	*C. porosus*	O79556	*L. semicarinatus*	O79678	*P.subrufa*
ND6	YP_637151.1	*C. porosus*	O79557	*L.semicarinatus*	O79679	*P. subrufa*
NRF1	XP_019399363.1	*C. porosus*	XP_033017880.1	*L.agilis*	XP_037745346.1	*C. mydas*
NRF2	XP_019409983.1	*C. porosus*	R4GBQ8	*A. carolinensis*	XP_037768003.1	*C. mydas*
NRIP1	XP_019384300.1	*C. porosus*	H9G4R0	*A. carolinensis*	XP_043394283.1	*C. mydas*
OPA1	XP_019388472.1	*C. porosus*	XP_033006830.1	*L.agilis*	XP_037765660.1	*C.mydas*
PARKIN	XP_019405532.1	*C.porosus*	XP_020664514.1	*P. vitticeps*	XP_037751044.1	*C.mydas*
PERM1	-	-	XP_033012172.1	*L. agilis*	XP_027688095.2	*C.mydas*
PINK1	-	-	XP_033012396.1	*L.agilis*	XP_037737240.1	*C. mydas*

POLG	XP_0193 89278.1	*C.porosus*	H9G560	*A. carolinensis*	XP_037767 462.1	*C.mydas*
POLG2	-	-	XP_03299 1802.1	*L.agilis*	XP_042696 945.1	*C.picta*
POLRMT	-	-	XP_02856 9394.1	*P. murallis*	XP_039371 953.1	*M.reevesii*
PMPCA	XP_0193 96476.1	*C. porosus*	H9GN03	*A.carolinensis*	XP_037735 395.1	*C.mydas*
PPARA	XP_0193 99827.1	*C. porosus*	XP_02064 1442.1	*P.vitticeps*	-	-
PPARD	XP_0194 02298.1	*C. porosus*	XP_03300 8560.1	*L. agilis*	XP_043389 468.1	*C.mydas*
PPARG	-	-	XP_03299 6680.1	*L.agilis*	XP_043407 765.1	*C.mydas*
PPARGC1A	XP_0194 08762.1	*C. porosus*	K7FZ84	*A.carolinensis*	XP_007058 167.2	*C. mydas*
PPARGC1B	XP_0193 90263.1	*C. porosus*	XP_03299 5783.1	*L.agilis*	XP_007057 303.2	*C. mydas*
PRC1	-	-	XP_03302 2567.1	*L.agilis*	XP_037766 206.1	*C. mydas*
PRKAA1	XP_0193 87541.1	*C. porosus*	XP_00810 1051.1	*A.carolinensis*	XP_007065 786.1	*C.mydas*
PRKAA2	XP_0193 86183.1	*C. porosus*	XP_03300 7910.1	*L. agilis*	XP_037763 652.1	*C. mydas*
SAMM50	XP_0193 99872.1	*C. porosus*	XP_02064 4569.1	*P. vitticeps*	XP_037770 688.1	*C.mydas*
SIRT1	XP_0193 94185.1	*C. porosus*	XP_00322 3739.1	*A.carolinensis*	XP_037759 905.1	*C.mydas*
SIRT3	XP_0194 02775.1	*C. porosus*	XP_02066 2646.1	*P. vitticeps*	XP_007063 942.1	*C. mydas*
SIRT4	XP_0193 94775.1	*C.porosus*	XP_03299 1953.1	*L.agilis*	XP_043385 514.1	*C.mydas*
SIRT5	XP_0193 99331.1	*C. porosus*	XP_02065 4256.1	*P.vitticeps*	XP_037749 007.1	*C. mydas*
SSBP1	XP_0194 00213.1	*C.porosus*	XP_03301 8966.1	*L. agilis*	XP_037734 852.1	*C. mydas*
SP1	XP_0194 10225.1	*C.porosus*	XP_02064 0162.1	*P.vitticeps*	XP_037739 697.1	*C.mydas*
SQSTM1	-	-	XP_02063 8407.1	*P. vitticeps*	XP_043408 524.1	*C.mydas*
TFAM	XP_0193 94126.1	*C. porosus*	XP_03300 5033.1	*L.agilis*	XP_037761 270.1	*C.mydas*

TFB1M	XP_019405595.1	*C. porosus*	XP_028579572.1	*P. murallis*	XP_043399122.1	*C.mydas*
TFB2M	XP_019405303.1	*C. porosus*	XP_033000289.1	*L. agilis*	XP_007058049.3	*C. mydas*
TRAK1	XP_019393014.1	*C. porosus*	XP_033021701.1	*L.agilis*	XP_027685352.2	*C. mydas*
TRAK2	XP_019409363.1	*C. porosus*	XP_033025502.1	*L.agilis*	XP_043381603.1	*C. mydas*
TWNK	-	-	XP_033005698.1	*L.agilis*	XP_007066971.3	*C. mydas*
ULK1	-	-	XP_020644507.1	*P. vitticeps*	XP_043385971.1	*C. mydas*
YY1	XP_019408054.1	*C. porosus*	XP_032995680.1	*L.agilis*	XP_027683116.2	*C. mydas*

Table S6 - Pseudogene information. Retrieved from exonerate outputs, which include information on sequences of a genome that are similar to the query sequence used.

Species	**Gene**	**Type**	**Location (aa)**	**Contig**
Actinemys marmorata	*ND3*	frame	59	VOGN01098713.1
Actinemys marmorata	*PPARA*	frame	48	VOGN01040940.1
Actinemys marmorata	*SQSTM1*	stop	63	VOGN01000126.1
Alectura lathami	*OPA1*	stop	588	VXAV01001746.1
Alligator sinensis	*MFN1*	frame	21	AVPB01061842.1
Alligator sinensis	*PPARD*	frame	10	AVPB01147821.1
Anolis carolinensis	*ANT2*	stop	68	AAWZ02035470.1
Anolis carolinensis	*MAP1B*	frame	864	AAWZ02003589.1
Anolis carolinensis	*TFB2M*	frame	70	AAWZ02029836.1
Anolis carolinensis	*TRAK1*	stop	144	AAWZ02002850.1
Anolis carolinensis	*TRAK1*	stop	302	AAWZ02020453.1
Anomalopteryx didiformis	*POLG*	frame	893	SZQC01000084.1
Anomalopteryx didiformis	*TFB1M*	frame	108	SZQC01000092.1
Anomalopteryx didiformis	*TWK*	frame	54	SZQC01000265.1
Anomalopteryx didiformis	*ULK1*	frame	635	SZQC01000157.1
Anseranas semipalmata	*POLG2*	stop	457	VXAA01003411.1
Apteryx owenii	*TFAM*	stop	18	PTFC01000463.1
Asarcornis scutulata	*MTOR*	frame	898	VZSO01000078.1
Asarcornis scutulata	*TFB1M*	frame	278	VZSO01000032.1
Aspidoscelis marmoratus	*ATP6*	stop	147	MTQE01003379.1
Aspidoscelis marmoratus	*COX2*	frame	199	MTQE01003116.1
Aspidoscelis marmoratus	*COX3*	stop	37	MTQE01003379.1
Aspidoscelis marmoratus	*ND1*	stop	167	MTQE01002494.1
Branta canadensis	*ANT1*	frame	14	SNRU01007508.1

Cairina moschata	*SP1*	stop	589	QZEJ01000517.1
Callipepla squamata	*PPARD*	frame	251	MCFN01000014.1
Chauna torquata	*POLG2*	stop	457	VXAL01006304.1
Chauna torquata	*PPARD*	frame	233	VXAL01014437.1
Chauna torquata	*TFAM*	frame	17	VXAL01017831.1
Chelonia mydas	*POLG2*	frame	60	JADCQM020000036.1
Chelonoidis abingdonii	*PPARGC1B*	stop	444	PKMU01003090.1
Chelydra serpentina	*PPARGC1B*	frame	829	JAHGAV010000001.1
Chelydra serpentina	*SAMM50*	frame	305	JAHGAV010001008.1
Chelydra serpentina	*SQSTM1*	stop	63	JAHGAV010000001.1
Chelydra serpentina	*ULK1*	stop	9	JAHGAV010000052.1
Chrysemys picta	*MAP1B*	frame	697	AHGY03018123.1
Chrysemys picta	*PPARGC1A*	frame	404	AHGY03013828.1
Chrysemys picta	*SIRT1*	frame	103	AHGY03032212.1
Chrysemys picta	*SQSTM1*	stop	63	AHGY03002094.1
Chrysemys picta	*ULK1*	frame	739	AHGY03098480.1
Chrysolophus pictus	*POLG2*	stop	457	JRFT01050193.1
Chrysolophus pictus	*PPARD*	frame	270	JRFT01010374.1
Chrysolophus pictus	*YY1*	frame	175	JRFT01064797.1
Colinus virginianus	*PPARD*	frame	218	AWGT02000210.1
Crocodylus porosus	*TWK*	stop	656	gi|1063923462|gb|MDVP01000069.1|
Crotalus viridis	*CHCHD3*	stop	106	PDHV02000002.1
Crotalus viridis	*COX3*	frame	73	PDHV02000003.1
Crypturellus cinnamomeus	*PPARD*	frame	214	PTEZ01000054.1
Crypturellus soui	*PPARD*	frame	214	VWPX01075051.1
Cuora mccordi	*SQSTM1*	stop	63	RQSS01025273.1
Cuora mccordi	*TFB1M*	stop	4	RQSS01014891.1
Cuora mccordi	*ULK1*	frame	38	RQSS01023015.1
Cygnus cygnus	*PPARD*	frame	232	BMBB01016471.1
Cygnus olor	*CCND1*	frame	155	WNMI01000005.1
Cygnus olor	*CREB1*	frame	114	WNMI01000006.1
Cygnus olor	*MTOR*	frame	356	WNMI01000021.1
Cygnus olor	*NRF2*	frame	154	WNMI01000006.1
Cygnus olor	*PINK1*	stop	183	WNMI01000021.1
Cygnus olor	*PPARD*	frame	232	WNMI01000024.1
Cygnus olor	*SAMM50*	frame	273	WNMI01000001.1
Cygnus olor	*SSBP1*	frame	52	WNMI01000001.1
Cygnus olor	*TRAK1*	frame	673	WNMI01000004.1
Dermochelys coriacea	*GSK3B*	frame	39	WSPL04000001.1
Emydocephalus ijimae	*CHCHD3*	stop	163	BHEV01133271.1
Emydocephalus ijimae	*TFAM*	stop	244	BHEV01113624.1
Eudromia elegans	*POLG2*	stop	475	PTEX01000049.1

Gavialis gangeticus	*MFN1*	frame	20	gi|1063925351|gb|MDVQ01000046.1|
Gavialis gangeticus	*PPARD*	frame	16	gi|1063923830|gb|MDVQ01000068.1|
Gekko japonicus	*SAMM50*	frame	13	LNDG01140238.1
Gopherus evgoodei	*OPA1*	frame	39	VHHN01000011.1
Gopherus evgoodei	*PPARG*	frame	21	VHHN01000349.1
Gopherus evgoodei	*PPARGC1A*	frame	766	VHHN01000327.1
Gopherus evgoodei	*ULK1*	frame	19	VHHN01000075.1
Hydrophis curtus	*MIEF1*	frame	19	JABAHG010000004.1
Hydrophis curtus	*POLRMT*	frame	694	JABAHG010000001.1
Hydrophis curtus	*PPARGC1A*	frame	153	JABAHG010000007.1
Hydrophis curtus	*SAMM50*	frame	226	JABAHG010000004.1
Hydrophis curtus	*TFAM*	stop	244	JABAHG010000004.1
Hydrophis curtus	*TRAK2*	frame	794	JABAHG010000001.1
Hydrophis curtus	*TWK*	frame	33	JABAHG010000004.1
Hydrophis cyanocinctus	*MIC10*	frame	61	JAAZTL010000017.1
Hydrophis cyanocinctus	*MIC13*	frame	66	JAAZTL010000001.1
Hydrophis cyanocinctus	*MTOR*	frame	886	JAAZTL010000017.1
Hydrophis cyanocinctus	*PPARA*	stop	35	JAAZTL010000004.1
Hydrophis cyanocinctus	*PPARGC1A*	frame	338	JAAZTL010000007.1
Hydrophis cyanocinctus	*TFAM*	stop	244	JAAZTL010000004.1
Hydrophis cyanocinctus	*TWK*	frame	102	JAAZTL010000004.1
Lagopus muta	*MIC13*	frame	42	BJCA01040788.1
Lagopus muta	*POLG2*	stop	457	BJCA01008947.1
Lagopus muta	*PPARD*	frame	254	BJCA01012997.1
Laticauda colubrina	*OPA1*	frame	42	BLBF01000076.1
Laticauda colubrina	*PPARGC1A*	stop	597	BLBF01000039.1
Laticauda colubrina	*TFAM*	stop	244	BLBF01000016.1
Mauremys mutica	*PPARA*	frame	49	JADWOL010000001.1
Mauremys mutica	*ULK1*	frame	38	NC_059087.1
Mauremys reevesii	*SQSTM1*	stop	63	JADWOL010000008.1
Meleagris gallopavo	*PRC1*	stop	88	ADDD02032772.1
Mesoclemmys tuberculata	*ND1*	stop	32	VOCS01058072.1
Mesoclemmys tuberculata	*ND1*	stop	32	VOCS01058072.1
Mesoclemmys tuberculata	*ULK1*	frame	68	VOCS01015983.1
Naja naja	*MTOR*	frame	548	SOZL01000219.1
Naja naja	*NCOR1*	frame	1429	SOZL01001084.1
Naja naja	*POLG2*	frame	109	SOZL01001309.1
Naja naja	*PPARA*	stop	35	SOZL01001622.1
Naja naja	*TFAM*	stop	243	SOZL01000003.1
Notechis scutatus	*PPARGC1A*	frame	556	ULFQ01000109.1

Notechis scutatus	*TFAM*	stop	244	ULFQ01000322.1
Nothocercus julius	*PPARD*	frame	215	VZSV01000183.1
Nothocercus nigrocapillus	*PPARD*	frame	215	WBNA01000577.1
Odontophorus gujanensis	*POLG2*	stop	457	VXAB01004361.1
Odontophorus gujanensis	*PPARD*	frame	308	VXAB01007058.1
Ophiophagus hannah	*TFAM*	stop	243	AZIM01002367.1
Pantherophis guttatus	*TFAM*	stop	181	JTLQ02000088.1
Pantherophis guttatus	*TRAK1*	stop	556	JTLQ02000222.1
Pantherophis obsoletus	*TFAM*	frame	227	WJSR01000027.1
Pantherophis obsoletus	*TRAK1*	stop	556	WJSR01000511.1
Pavo cristatus	*MIC13*	frame	40	QZWQ01000116.1
Pavo cristatus	*POLG2*	stop	457	QZWQ01001636.1
Pavo cristatus	*PPARD*	stop	216	QZWQ01000248.1
Pavo muticus	*MIC13*	frame	40	JACDJE010000387.1
Pavo muticus	*MIEF2*	stop	138	JACDJE010000022.1
Pavo muticus	*POLG*	stop	1026	JACDJE010000002.1
Pavo muticus	*POLG2*	stop	457	JACDJE010000038.1
Pavo muticus	*PPARD*	stop	216	JACDJE010000053.1
Pavo muticus	*SIRT3*	stop	19	JACDJE010000197.1
Pelodiscus sinensis	*ANT3*	stop	34	AGCU01170808.1
Pelodiscus sinensis	*POLRMT*	stop	879	AGCU01077855.1
Pelodiscus sinensis	*SP1*	stop	51	AGCU01201756.1
Pelusios castaneus	*PINK1*	frame	157	VOCT01019444.1
Penelope pileata	*PPARD*	frame	215	WBMW01001137.1
Penelope pileata	*PPARG*	frame	84	WBMW01003833.1
Penelope pileata	*TFAM*	stop	5	WBMW01006495.1
Pituophis catenifer	*TFAM*	frame	227	JAHUAB010000005.1
Platysternon megacephalum	*SQSTM1*	stop	63	QXTE01000051.1
Podarcis muralis	*MFN2*	frame	671	SIRZ01000008.1
Podarcis muralis	*MIEF1*	frame	16	SIRZ01000010.1
Podarcis muralis	*OPA1*	frame	543	SIRZ01000005.1
Pseudonaja textilis	*TFAM*	stop	182	ULFR01000062.1
Ptyas mucosa	*TRAK1*	stop	556	WNWU01013587.1
Python bivittatus	*SIRT5*	stop	302	AEQU02223380.1
Sceloporus undulatus	*MIRO2*	frame	82	JAGXEY010000008.1
Sceloporus undulatus	*PRKAA2*	frame	121	JAGXEY010000004.1
Sphenodon punctatus	*ANT3*	stop	194	QEPC01003743.1
Sphenodon punctatus	*CREB1*	stop	175	QEPC01000089.1
Sphenodon punctatus	*MAP1B*	stop	688	QEPC01000724.1
Sphenodon punctatus	*MFN1*	stop	654	QEPC01012362.1
Sphenodon punctatus	*YY1*	stop	273	QEPC01002847.1
Stictonetta naevosa	*PPARD*	frame	233	JAACYO010007055.1

Syrmaticus mikado	*MIC13*	frame	39	QGNR01000137.1
Syrmaticus mikado	*POLG2*	stop	457	QGNR01000021.1
Syrmaticus mikado	*PPARD*	frame	268	QGNR01000073.1
Syrmaticus mikado	*PPARG*	frame	85	QGNR01000008.1
Terrapene carolina	*MTOR*	stop	83	PRFB02000715.1
Terrapene carolina	*SQSTM1*	stop	63	PRFB02000630.1
Thamnophis elegans	*NRIP1*	frame	448	WNNA01000350.1
Thamnophis elegans	*TRAK2*	frame	353	WNNA01000208.1
Thermophis baileyi	*TRAK1*	stop	556	QLTV01000029.1
Trachemys scripta	*SIRT1*	frame	258	VIRI01000007.1
Trachemys scripta	*SQSTM1*	stop	63	VIRI01000008.1
Tympanuchus cupido	*MIC13*	frame	25	gi|1100818802|gb|MOXI01000150.1|
Tympanuchus cupido	*POLG2*	stop	457	gi|1100818823|gb|MOXI01000129.1|
Tympanuchus cupido	*PPARD*	frame	255	gi|1100818911|gb|MOXI01000041.1|
Tympanuchus cupido	*PPARG*	frame	86	gi|1100818915|gb|MOXI01000037.1|
Vipera berus	*TFAM*	stop	244	JTGP01189419.1
Zootoca vivipara	*MIRO1*	frame	624	JAATIO010000001.1
Zootoca vivipara	*MTOR*	frame	121	JAATIO010000002.1
Zootoca vivipara	*NRF1*	frame	379	JAATIO010000014.1

Table S7 - Selected metrics of codon usage bias and softwares used in their calculation

Metric	**Calculated with**
Codon Adaptative Index (CAI)	CAIcal webserver [95]
Effective number of codons (ENC)	DNASP [79]
Scaled chi squared (Schi2)	DNASP [79]
Relative Synonymous Codon Usage (RSCU)	DNASP [79]
Guanine-cytosine content (GC)	DNASP [79]
Guanine and cytosine content at the third codon position (GC3)	DNASP [79]

Table S8 - Phenotype continuous and categorical traits retrieved from available databases.

Phenotype trait	**Databases used**
Average adult body mass	Avibase Avibase [154]; Amniota [155]; AnAge [156]; [157]; [158]; [159]
Average annual environmental temperature at centroid location	Wolfram|Alpha [160]
Average body temperature	AnAge [156]; [158]; [159]
Basal and standard metabolic rate	AnAge [156]; [161]; [159]
Centroid latitude	Avibase Avibase [154]; [157]
Primary lifestyle	[157]; IUCN red list [162]
Habitat	Avibase Avibase [154]; IUCN red list [162]
Trophic level	Avibase Avibase [154]
Migratory strategy	Avibase Avibase [154] IUCN red list [162]

Table S9 - Models tested in jModeltest software for the concatenated dataset.

Model	-lnL	K	AICc	Delta	Weight	Cum Weight
GTR+I+G	303277.290	180	606916.840	0.000	1.000	1.000
SYM+I+G	303408.690	177	607173.550	256.720	1.800E-56	1.000
HKY+I+G	303583.240	176	607520.630	603.790	7.730E-132	1.000
K80+I+G	303717.430	173	607782.950	866.110	8.430E-189	1.000
GTR+G	304507.140	179	609374.520	2457.680	0.000	1.000
SYM+G	304676.440	176	609707.040	2790.200	0.000	1.000
HKY+G	304909.000	175	610170.130	3253.290	0.000	1.000
K80+G	305045.280	172	610436.620	3519.790	0.000	1.000
GTR+I	312825.220	179	626010.660	19093.830	0.000	1.000
SYM+I	313007.010	176	626368.180	19451.340	0.000	1.000
HKY+I	313033.050	175	626418.230	19501.390	0.000	1.000
K80+I	313237.570	172	626821.200	19904.370	0.000	1.000
F81+I+G	321919.930	175	644192.000	37275.170	0.000	1.000
JC+I+G	322055.940	172	644457.950	37541.110	0.000	1.000
F81+G	323141.110	174	646632.330	39715.490	0.000	1.000
JC+G	323283.920	171	646911.880	39995.050	0.000	1.000
F81+I	331007.330	174	662364.770	55447.940	0.000	1.000
JC+I	331141.730	171	662627.500	55710.660	0.000	1.000
GTR	334713.260	178	669784.730	62867.900	0.000	1.000
SYM	334852.660	175	670057.460	63140.630	0.000	1.000
HKY	335069.590	174	670489.290	63572.450	0.000	1.000
K80	335192.030	171	670728.090	63811.260	0.000	1.000
F81	352625.190	173	705598.460	98681.630	0.000	1.000
JC	352779.740	170	705901.500	98984.660	0.000	1.000

Table S10 - Selected model of evolution for the 101 partitions

Partition	Gene	Model of evolution	Proportion of invariable sites	Gamma shape
1	*ANT1*	SYM+I+G	0.499	0.949
2	*ANT2*	HKY+I+G	0.512	1.086
3	*ANT3*	GTR+I+G	0.479	1.181
4	*ATP6*	GTR+I+G	0.18	0.584
5	*ATP8*	GTR+I+G	0	0.346
6	*CAMK4*	K80+I+G	0.294	0.8
7	*CCND1*	SYM+I+G	0.417	0.698
8	*CHCHD3*	GTR+G	-	0.566
9	*COX1*	GTR+I+G	0.399	0.408
10	*COX2*	GTR+I+G	0.349	0.465
11	*COX2*	GTR+I+G	0.246	0.489
12	*COX3*	GTR+I+G	0.318	0.496
13	*CREB1*	HKY+I+G	0.573	1.459
14	*CYTB*	GTR+I+G	0.227	0.486
15	*DNM1L*	GTR+I+G	0.47	1.482
16	*DNM1L*	K80+G	-	0.258
17	*ESRRB*	HKY+I+G	0.575	1.155
18	*ESRRG*	SYM+I+G	0.447	0.639
19	*FUNDC1*	K80+G	-	0.264
20	*FUNDC1*	GTR+I+G	0.512	1.082
21	*GSK3B*	SYM+I+G	0.341	0.677
22	*GSK3B*	K80+G	-	0.537
23	*MAP1B*	JC	-	-
24	*MAP1B*	HKY+I+G	0.339	1.577
25	*MAP1B*	K80+G	-	0.264
26	*MFF*	HKY+I+G	0.317	0.731
27	*MFN1*	HKY+I+G	0.473	1.344
28	*MFN1*	GTR+I+G	0.26	0.979
29	*MFN2*	GTR+I+G	0.494	1.19
30	*MIC10*	K80+G	-	0.406
31	*MIC13*	K80+G	-	0.711
32	*MIC60*	GTR+I+G	0.219	1.137
33	*MIC60*	GTR+I+G	0.312	1.046
34	*MIEF1*	K80+I+G	0.428	1.794
35	*MIEF2*	GTR+I+G	0.118	1.215

36	*MIRO1*	SYM+I+G	0.307	0.842
37	*MIRO1*	HKY+I+G	0.438	1.205
38	*MIRO2*	HKY+I+G	0.473	0.778
39	*MIRO2*	HKY+I+G	0.219	0.922
40	*MTERF2*	GTR+I+G	0.163	1.776
41	*MTOR*	GTR+I+G	0.163	1.776
42	*MTOR*	GTR+I+G	0.58	1.459
43	*MTX2*	SYM+G	-	0.427
44	*NCOR1*	HKY+I+G	0.501	0.802
45	*NCOR1*	GTR+I+G	0.4	0.971
46	*ND1*	GTR+I+G	0.261	0.484
47	*ND2*	GTR+I+G	0.091	0.535
48	*ND3*	GTR+I+G	0.263	0.375
49	*ND4*	GTR+I+G	0.197	0.534
50	*ND4L*	HKY+G	-	0.477
51	*ND5*	GTR+I+G	0.215	0.532
52	*ND5*	GTR+I+G	0.026	0.59
53	*ND6*	HKY+G	-	0.502
54	*NRF2*	GTR+I+G	0.219	1.749
55	*NRIP1*	HKY+I+G	0.346	1.288
56	*NRIP1*	GTR+I+G	0.127	1.477
57	*OPA1*	GTR+I+G	0.421	1.35
58	*OPA1*	K80+I+G	0.471	1.372
59	*PARKIN*	GTR+I+G	0.239	1.212
60	*PINK1*	HKY+I+G	0.24	1.285
61	*PMPCA*	F81+G	-	0.598
62	*PMPCA*	GTR+I+G	0.417	1.183
63	*POLG*	GTR+I+G	0.363	1.304
64	*POLG2*	GTR+I+G	0.203	1.001
65	*POLRMT*	HKY+I+G	0.153	1.874
66	*POLRMT*	HKY+I+G	0.26	0.908
67	*PPARA*	GTR+I+G	0.493	1.546
68	*PPARD*	SYM+I+G	0.496	1.25
69	*PPARG*	GTR+G	-	0.441
70	*PPARG*	HKY+I+G	0.259	0.529
71	*PPARGC1A*	GTR+I+G	0.207	1.097
72	*PPARGC1B*	SYM+G	-	0.613
73	*PPARGC1B*	HKY+I+G	0.139	1.885
74	*PPARGC1B*	SYM+I+G	0.218	1.243

75	*PRC1*	GTR+I+G	0.17	1.235
76	*PRKAA1*	GTR+I+G	0.423	0.919
77	*PRKAA2*	GTR+I+G	0.472	0.907
78	*PRKAA2*	K80+G	-	0.409
79	*SAMM50*	GTR+I+G	0.486	1.424
80	*SIRT1*	GTR+I+G	0.427	1.257
81	*SIRT1*	K80+I+G	0.24	2.991
82	*SIRT3*	HKY+I+G	0.339	2.064
83	*SIRT5*	GTR+I+G	0.355	1.476
84	*SP1*	GTR+G	-	0.424
85	*SP1*	HKY+I+G	0.378	1.514
86	*SP1*	HKY+G	-	0.414
87	*SQSTM1*	GTR+I+G	0.291	1.701
88	*SSBP1*	K80+I+G	0.404	1.159
89	*TFAM*	GTR+I+G	0.132	2.075
90	*TFB1M*	HKY+I+G	0.254	1.375
91	*TFB2M*	GTR+I+G	0.077	1.396
92	*TRAK1*	HKY+I+G	0.373	0.936
93	*TRAK1*	K80+I+G	0.351	1.086
94	*TRAK2*	JC	-	-
95	*TRAK2*	HKY+I+G	0.188	1.491
96	*TWK*	HKY+I+G	0.217	1.34
97	*TWK*	GTR+I+G	0.352	1.152
98	*ULK1*	SYM+I+G	0.45	1.022
99	*ULK1*	K80+G	-	0.293
100	*ULK1*	GTR+I+G	0.272	0.85
101	*YY1*	GTR+I+G	0.543	0.917

Table S11 - Spearman correlations between genetic factors of the genes that regulate the mitochondrial function and phenotypic traits related with endothermy. Significant values are shown in bold. ** Correlation is significant at the 0.01 level (2-tailed). * Correlation is significant at the 0.05 level (2-tailed).

		Mean body mass (g)	**Mean body temperature (ºC)**	**Distance to equator (º)**	**Annual average environmental temperature (ºC)**	**Basal metabolic rate (standardize)**
dS	Correlation Coefficient	-0.011	0.018	**-.031***	**.038****	-0.031
	N	6297	4582	6420	6300	2713
dN	Correlation Coefficient	-0.016	**-,032***	-0.015	0.021	-0.034
	N	6304	4588	6427	6306	2715
ω	Correlation Coefficient	-0.017	**-.078****	-0.007	0.003	-0.032
	N	6296	4581	6419	6299	2712
ENC	Correlation Coefficient	**-.044****	**-.048****	0.009	-0.004	**-.041***
	N	6367	4646	6492	6371	2761
Schi2	Correlation Coefficient	**.043****	**.053****	-0.005	-0.001	**.047***
	N	6367	4646	6492	6371	2761
GC	Correlation Coefficient	-0.010	**.169****	0.021	-0.022	**.054****
	N	6367	4646	6492	6371	2761
GC3	Correlation Coefficient	-0.019	**.161****	0.017	-0.021	**.045***
	N	6367	4646	6492	6371	2761
CAI *Gallus gallus*	Correlation Coefficient	-0.016	**.087****	0.016	-0.018	0.007
	N	6367	4646	6492	6371	2761
CAI *Pogona vitticeps*	Correlation Coefficient	-0.004	**.038****	0.012	-0.002	-0.011
	N	6367	4646	6492	6371	2761

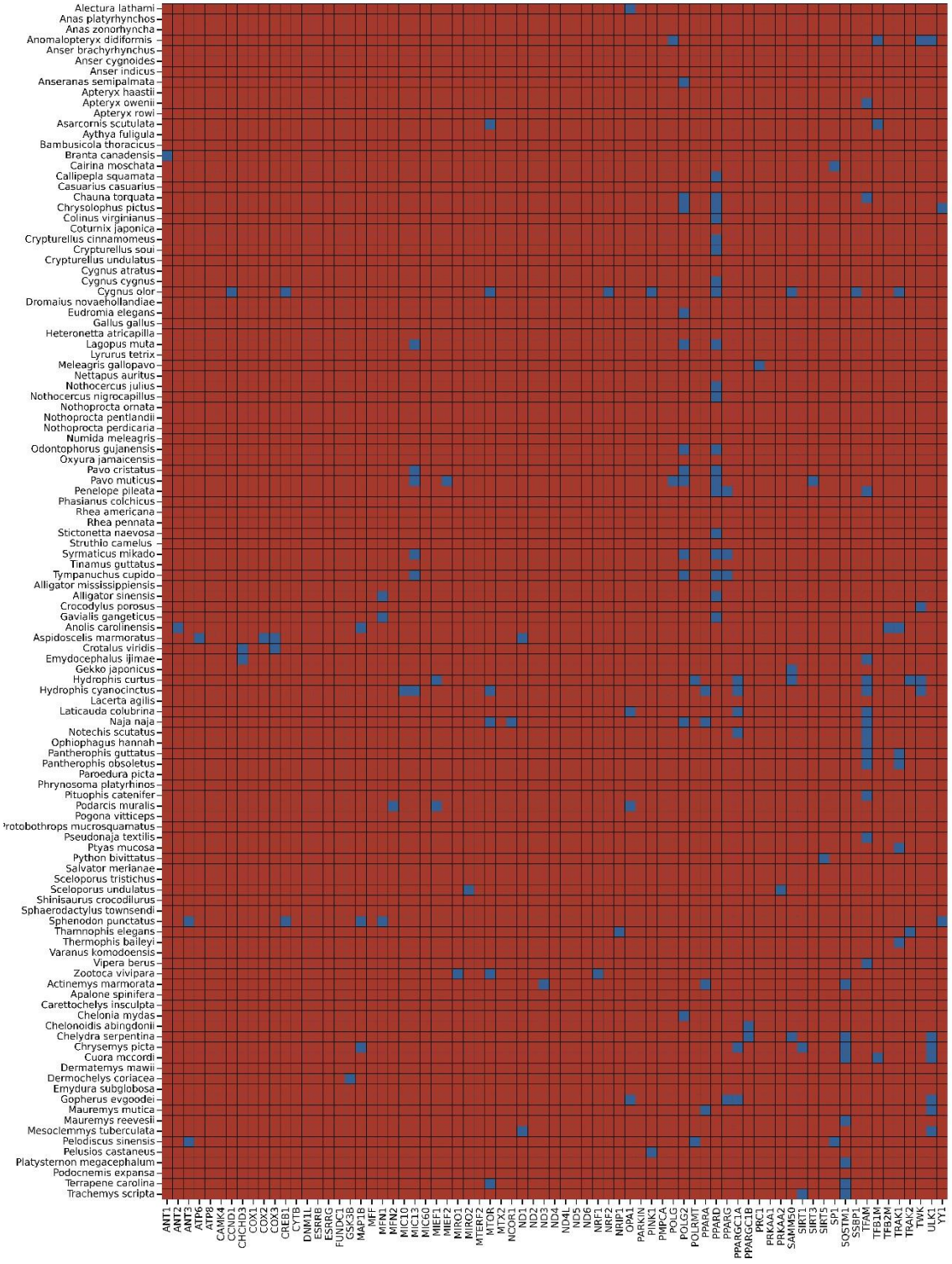

Figure S1 - Significant high correlations (R> 0.70) between basal metabolic rate (BMR) and genotype traits found of the genes that regulate the mitochondrial function.

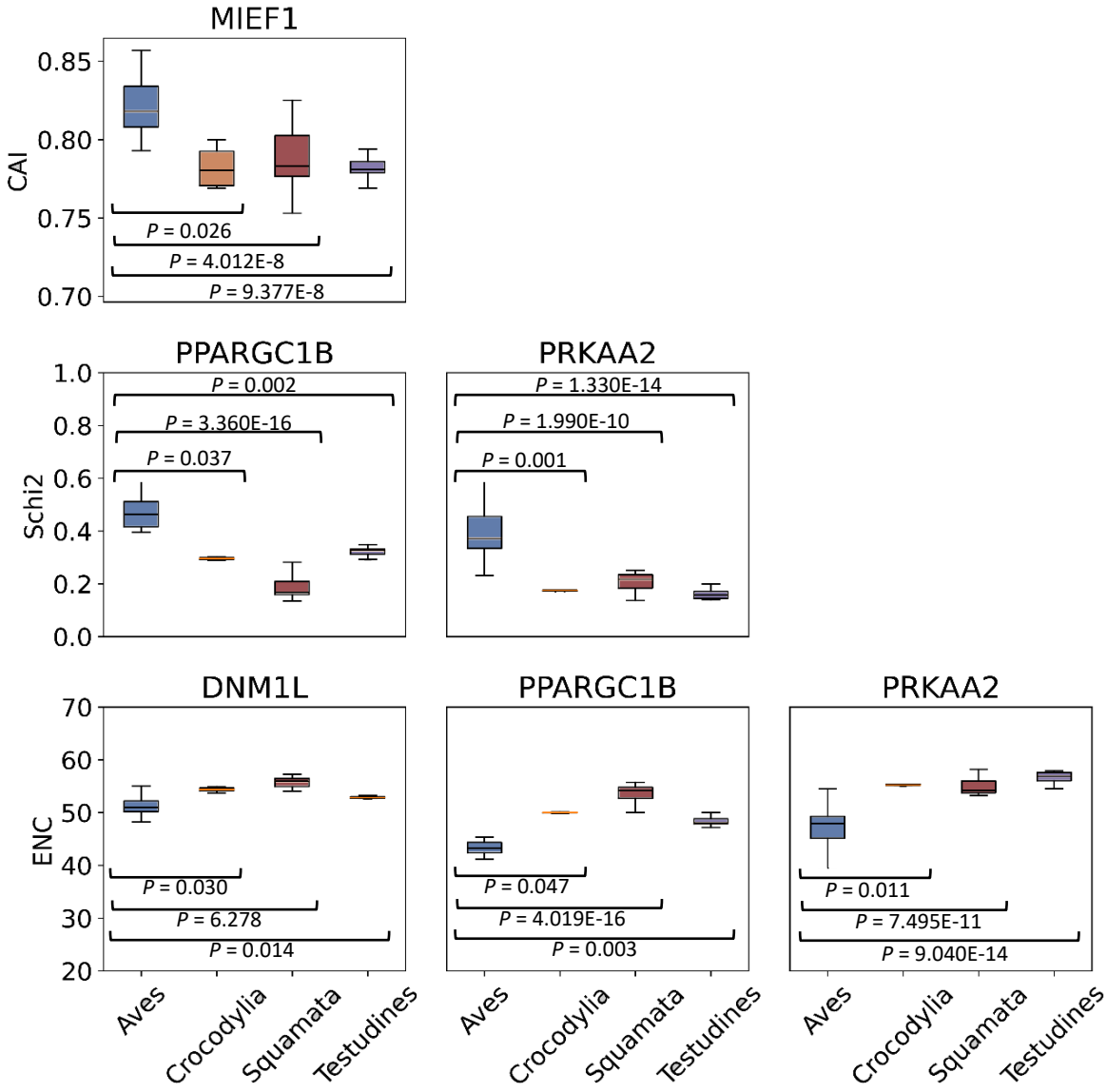

Figure S2 - Genes with significantly higher codon usage bias in birds than in each of the reptile orders. The p-values presented correspond to Tukey test p-values.

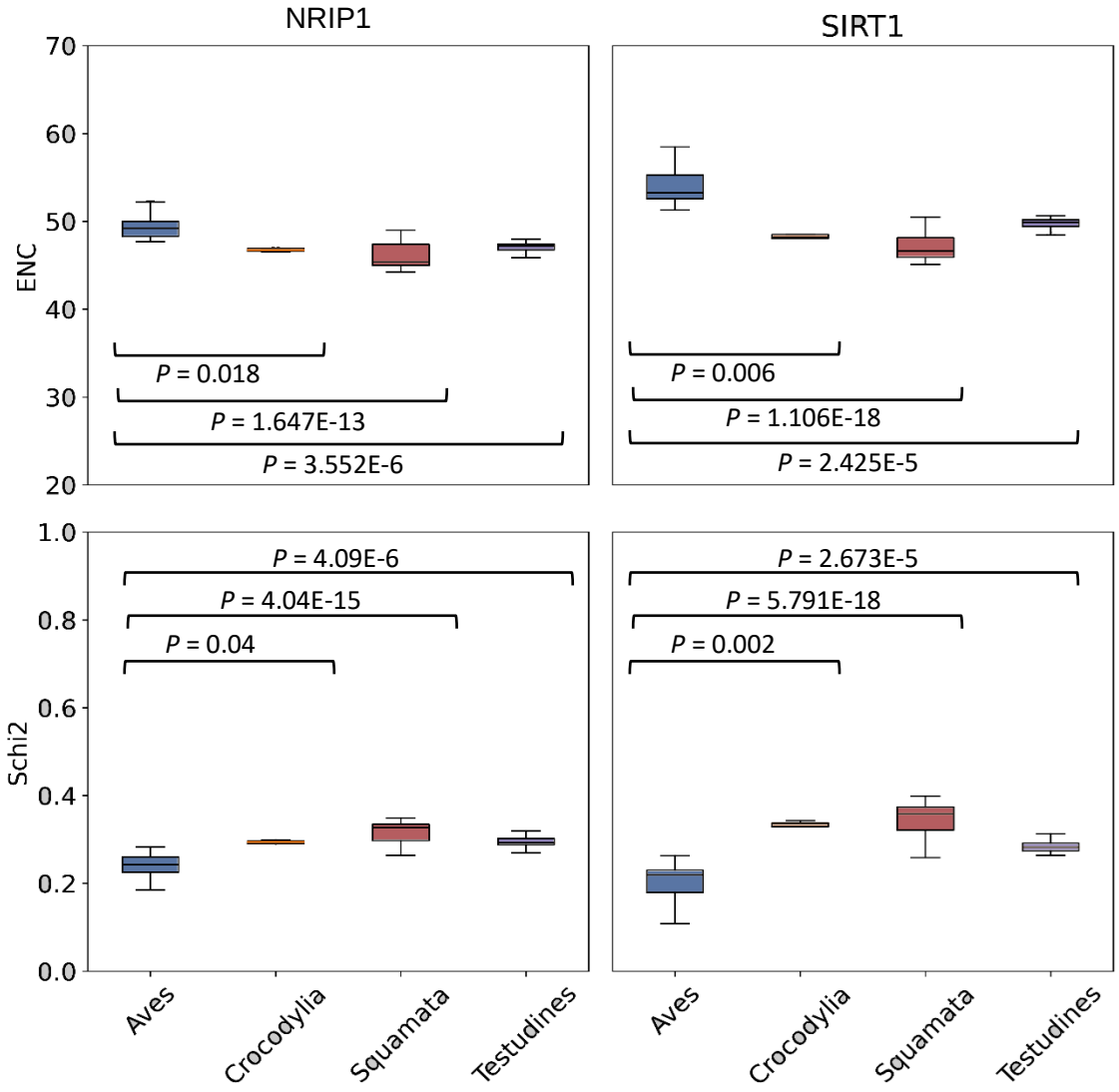

Figure S3 - Genes with significantly higher codon usage bias in reptiles than in birds. The p-values presented correspond to Tukey test p-values.

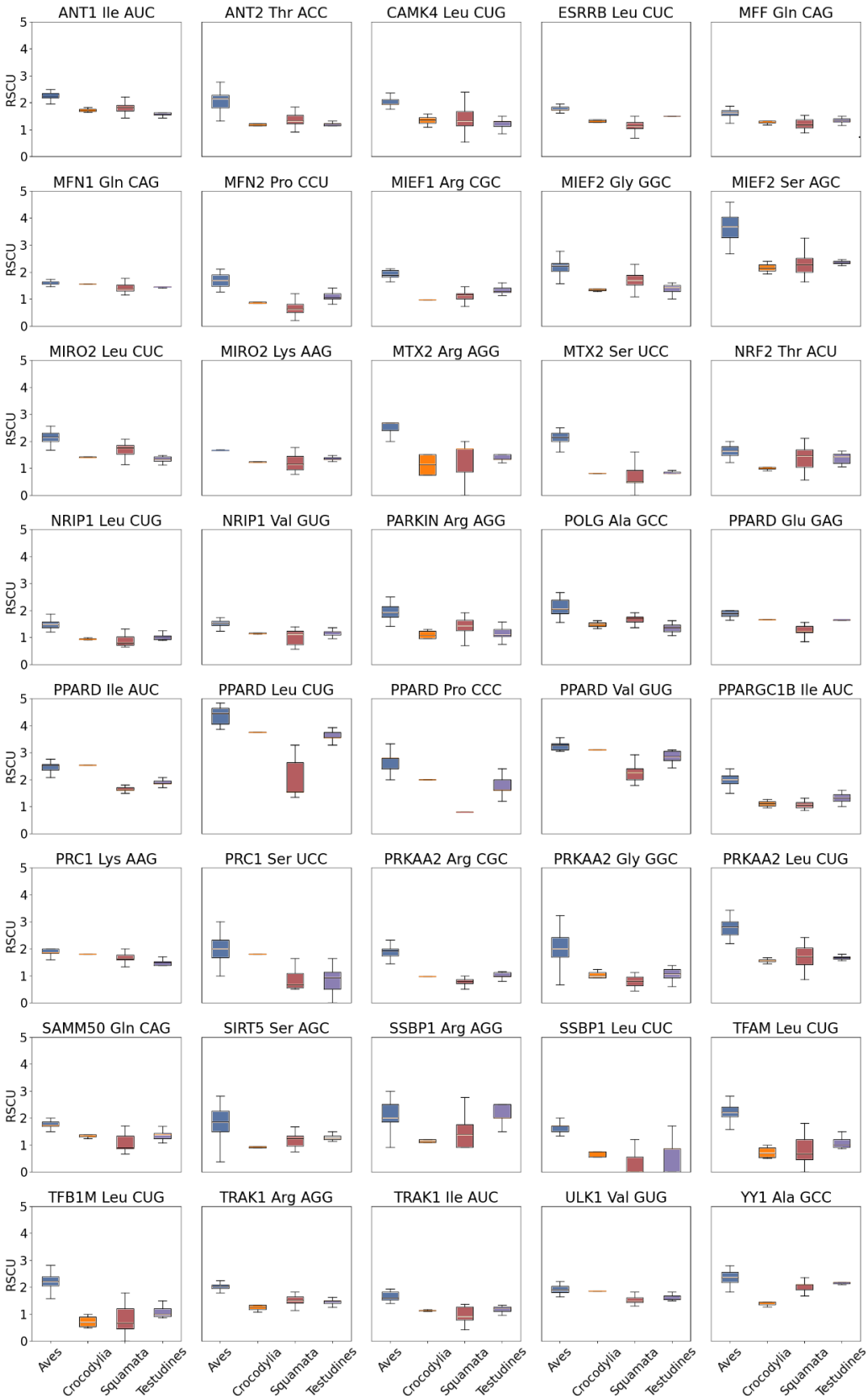

Figure S4 - Significant biased codons with significantly higher codon usage bias in birds than in each of the reptile orders, according to the RSCU metric.

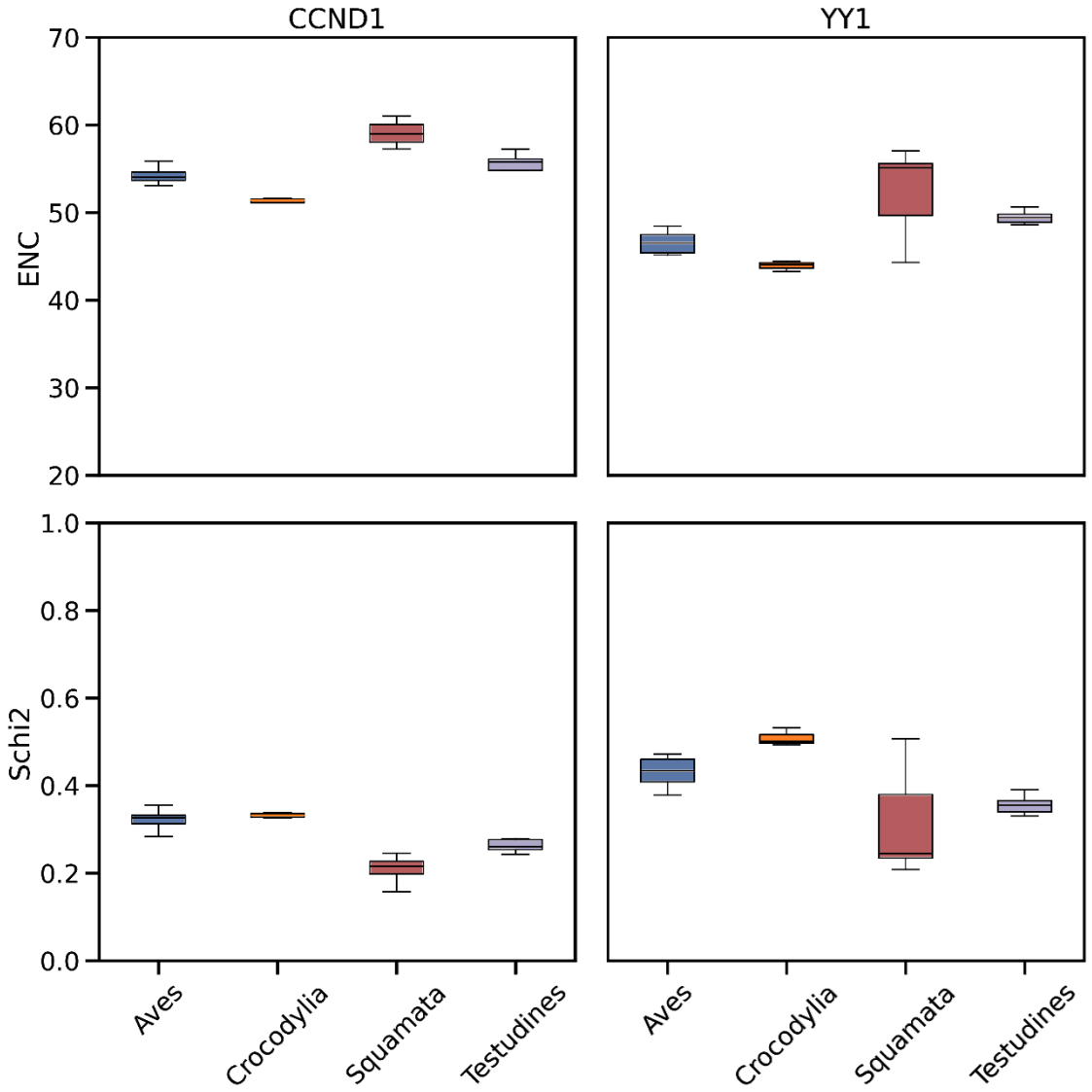

Figure S5 - Genes with significantly higher codon usage Archosauria than in Squamata or Testudines. The p-values presented correspond to Tukey test p-values.

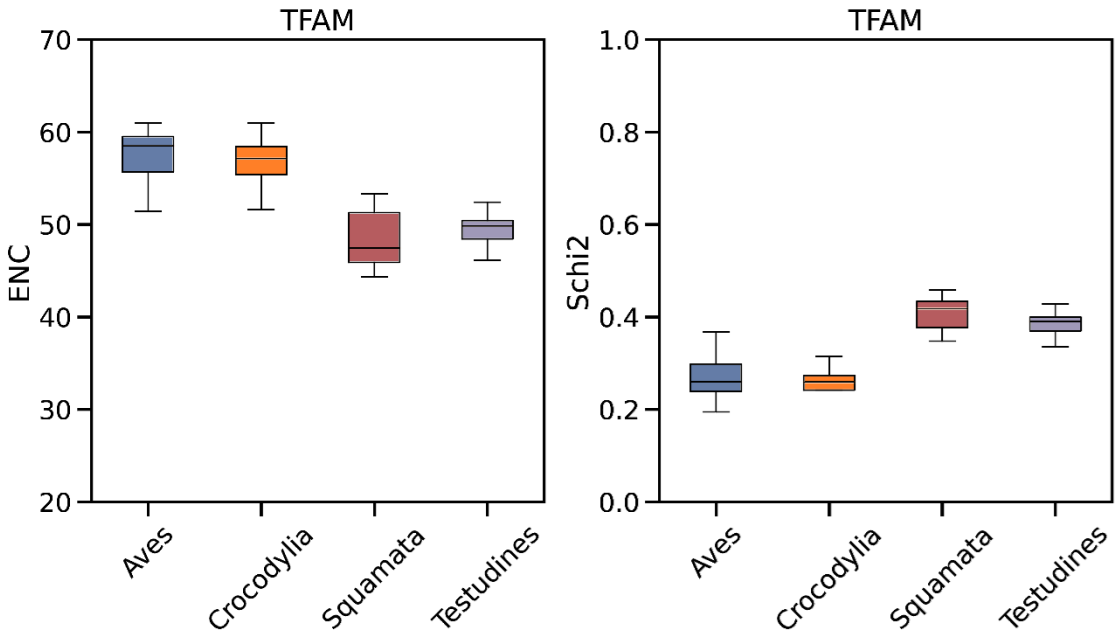

Figure S6 - Gene with significantly higher codon usage Squamata and Testudines than in the Archosauria. The p-values presented correspond to Tukey test p-values.

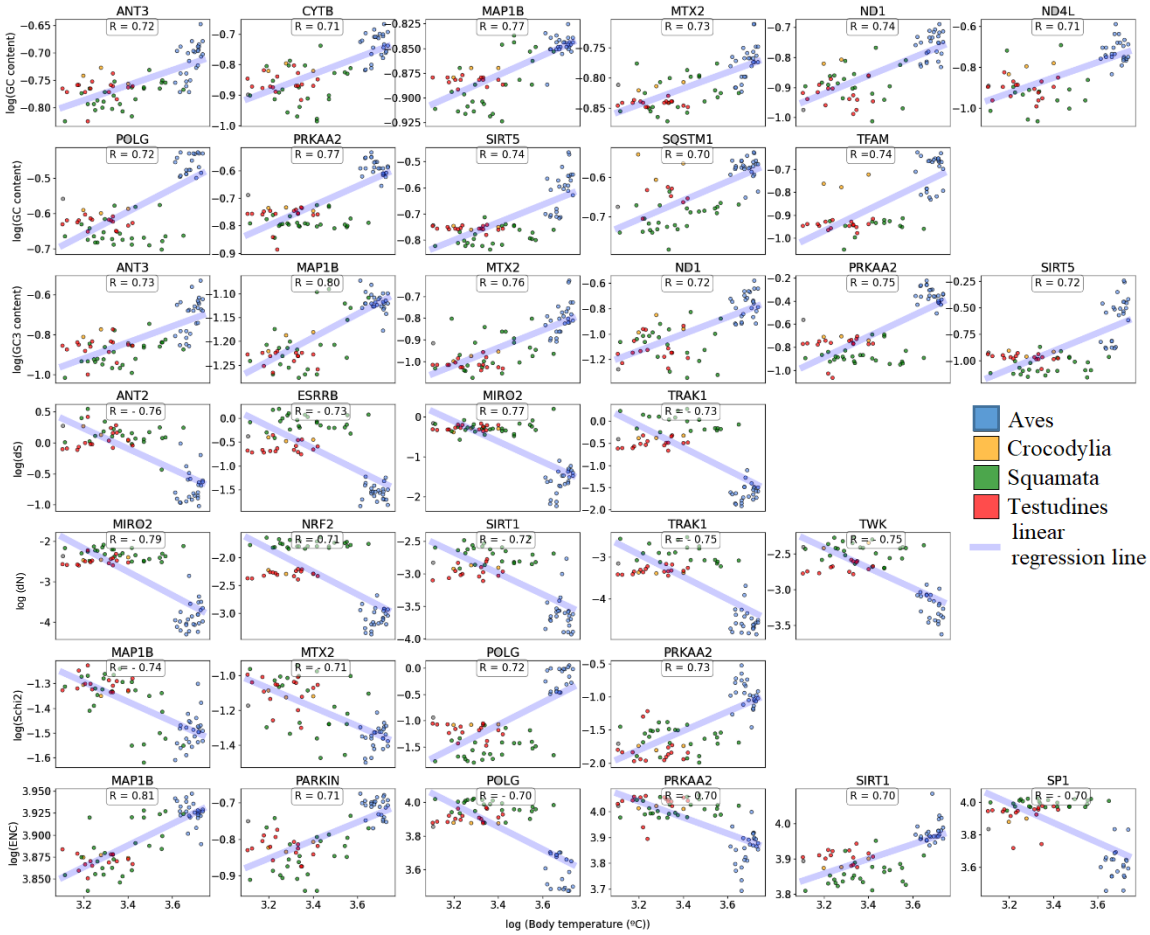

Figure S7 - Significant high correlations (R> 0.70) between body temperature and genotype traits found for the genes that regulate the mitochondrial function

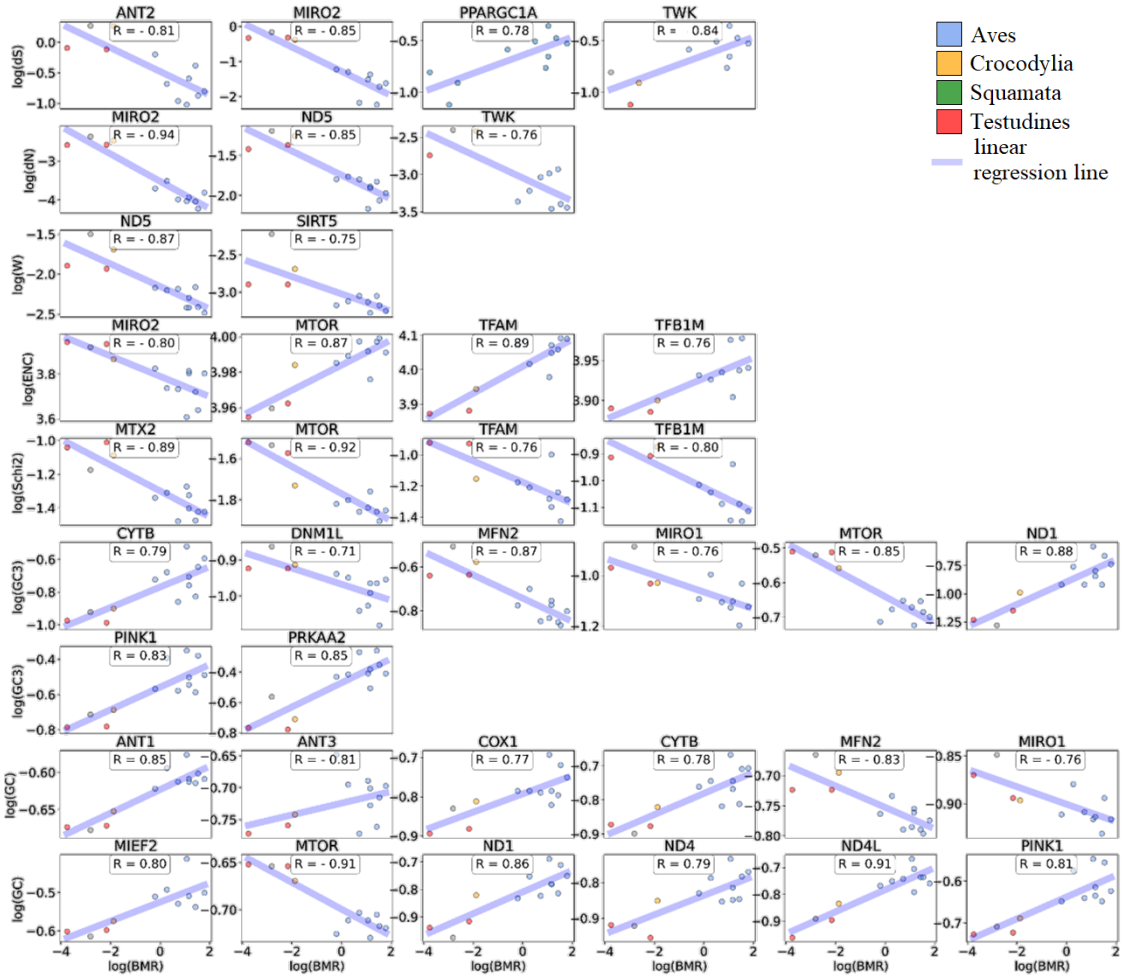

Figure S8 - Significant high correlations (R> 0.70) between basal metabolic rate (BMR) and genotype traits found of the genes that regulate the mitochondrial function.